https://doi.org/10.5194/egusphere-2026-6891
Preprint. Discussion started: 19 November 2026
© Author(s) 2026. CC BY 4.0 License.

Modeling new particle formation in the remote marine atmosphere using a nitric acid-based nucleation scheme in WRF-Chem

Romain Salignat[1], Sandra Banson[1], Aurelia Lupascu[2], Karine Sellegri[1], Clémence Rose[1]

[1]Université Clermont Auvergne, CNRS, Laboratoire de Météorologie Physique (LaMP), F-63000 Clermont-Ferrand, France
[2]ECMWF, Bonn, Germany

Correspondence to: Clémence Rose (c.rose@opgc.fr); Karine Sellegri (k.sellegri@opgc.fr)

Abstract. New particle formation (NPF) is a key source of cloud condensation nuclei over most oceans. Although sulfuric acid (H_2SO_4), primarily derived from the oxidation of dimethyl sulfide emitted by marine biota, is widely recognized as critical precursor for marine NPF, current nucleation schemes in models are based on theoretical formulations or continental observations, as no scheme has yet been developed specifically for the remote marine atmosphere. Recently, observations acquired in the southwest Pacific Ocean suggested that nighttime nucleation in pristine marine environments may instead be driven by nitrate ions (NO_3^-). Building on this, a nitric acid (HNO_3)-based nucleation parameterization has been developed, using HNO_3 as a proxy for NO_3^-. In this study, we tested and evaluated this new scheme against the default WRF-Chem Binary and Activation schemes, both relying on H_2SO_4 concentrations. Our analysis focused on marine nucleation events identified with a marine-specific criterion during the Sea2Cloud campaign, performed off New Zealand in biologically active waters of the Chatham Rise region. Simulations revealed that H_2SO_4-based schemes failed to reproduce the observed particle concentrations in the 1 to 10 nm diameter range, both in terms of magnitude and temporal variability. In contrast, the new HNO_3-based scheme performed significantly better under predominantly pristine marine conditions. These results highlight nitrate-driven nucleation as a promising alternative to sulfuric acid-based schemes in remote marine environments. Future work should be aimed at testing and validating this parameterization across other oceanic regions and atmospheric layers, including in particular the free troposphere, to fully assess its robustness.

1 Introduction

Marine aerosol particles are a core component of the climate system. They play a crucial role in marine cloud formation, providing a source of cloud condensation nuclei (CCN) for cloud droplet nucleation, thereby influencing cloud properties and, ultimately, radiative forcing (Twomey, 1977; Albrecht, 1989). Although marine aerosols have a potentially significant role in future climate change, the lack of knowledge on emissions processes, marine aerosols formation, and associated effects, contribute to large uncertainties in past and future climate projections (Carslaw et al., 2013, 2017; Brooks and Thornton, 2018, Bellouin et al., 2020).

https://doi.org/10.5194/egusphere-2026-6891
Preprint. Discussion started: 19 November 2026
© Author(s) 2026. CC BY 4.0 License.

Besides primary marine particles, which are emitted under sufficiently high wind speeds (Russel, et al., 2023; Song et al., 2023), another important source of CCN over the oceans is new particle formation (Merikanto et al., 2009; Gordon et al., 2017), especially in pristine environments (Brean et al., 2021). The new particle formation (NPF) process starts with the nucleation of highly condensable gas-phase precursors into cluster particles of approximately 1 nm diameter (Kerminen et al., 2018). These nanoparticles further grow into larger sizes until they eventually reach climatically significant sizes (Kulmala et al., 2004; Kerminen et al., 2018). Such NPF events have already been observed in the marine open ocean (Petters et al., 2006; O'Dowd et al., 2010; Shen et al., 2020; Brean et al., 2021; Peltola et al., 2023), or in coastal or sea-ice influenced air masses (O'Dowd et al., 2002; Collins et al., 2017; Jokinen et al., 2018; Beck et al., 2021; Baccarini et al., 2021), yet the nature and origin of gas-phase particle precursors involved in marine nucleation and growth remain unclear due to the paucity of observations.

Traditionally, sulfuric acid (H_2SO_4) is commonly accepted as a key driver of NPF (Kulmala and Laaksonen, 1990; Kulmala et al., 2004, 2013), including over open oceans (Fitzgerald, 1991), due to its very low vapor pressure in atmospheric conditions. Precisely, in the remote marine ocean, dimethyl sulfide (DMS), a biogenic volatile compound derived from phytoplankton productivity is considered the largest source of H_2SO_4 and methanesulfonic acid in the global atmosphere (Bates et al., 1987; Hulswar et al., 2022). Thereby, the biogeochemical cycle of DMS is thought to play a significant role in the Earth's climate system, leading to a hypothesized feedback loop between phytoplankton and cloud albedo (known as the CLAW hypothesis; Charlson et al., 1987). Nevertheless, this hypothesis has not been proven (Quinn & Bates, 2011), and observations in the marine atmosphere suggest that other species emitted by oceanic biological productivity may also contribute to NPF such as iodine (O'Dowd et al., 2002; Allan et al., 2015; Sipilä et al., 2016; Peltola et al., 2023), ammonia (Jokinen et al., 2018) and amines (Dall'Osto et al., 2012; Brean et al., 2021). However, these last observations suffer from possible coastal or sea-ice influences, and the chemical mechanisms occurring during open ocean nucleation is still under debate. Recently, Chamba et al. (2023) reported the occurrence of nitrate-driven nighttime nucleation from open ocean emissions based on measurements performed in Air-Sea Interaction Tanks over the Southwest Pacific Ocean during the Sea2Cloud campaign (Sellegri et al., 2023a). These experimental findings were tested and complemented using a box-model modeling approach in Salignat et al. (accepted), in which the probable biological origin of nitric acid, used as a proxy for nitrate ions, was investigated and constrained, and the associated nucleation mechanism formalized. These findings open a new horizon in marine aerosol research, suggesting a previously unrecognized contribution of atmospheric nitrate ions of marine biogeochemical origin in driving nighttime nucleation over the remote ocean, which relevance needs to be evaluated using 3D meso-scale realistic modeling. As discussed in Chamba et al. (2023), the possible role of nitrate ions in marine nucleation has likely been overlooked so far due to the instrumentation deployed for the chemical characterization of the newly formed clusters and their precursors, which often uses nitrate-based chemical ionization (Sipilä et al., 2016; Baccarini et al., 2021; Beck et al., 2021; Brean et al., 2021). Here, we test the plausibility of the hypothesis proposed in Chamba et al. (2023).

https://doi.org/10.5194/egusphere-2026-6891
Preprint. Discussion started: 19 November 2026
© Author(s) 2026. CC BY 4.0 License.

However, DMS is the primary and often the only marine biogenic precursor of sulfate and NPF implemented in atmospheric and climatic models (Séférian et al., 2019; Carslaw et al., 2013; Fiddes et al., 2021; Marelle et al., 2021; Bock et al., 2021). Most modeling studies usually use nucleation mechanisms based on sulfuric acid concentrations, such as the theoretical binary (H_2SO_4-H_2O) nucleation (Vehkamaki et al., 2002; Wexler et al., 1994) and ternary (H_2SO_4-NH_3-H_2O) nucleation (Merikanto et al., 2007; Napari et al., 2002) schemes, or otherwise the empirical nucleation rates that use the first- (A * [H_2SO_4]) or second-order (A * [H_2SO_4]^2) parameterization (Kuang et al., 2008; Wang and Penner, 2009). Binary nucleation alone cannot explain the highest nucleation rates observed in the marine boundary layer (Weber et al., 1999), and is not predicted to occur under realistic conditions, unless in the cold upper troposphere as shown by global models (Lucas and Akimoto, 2006; Dunne et al., 2016), or polar air masses with a box model (Pirjola et al., 2000). On the other hand, ternary nucleation with ammonia in the system, supposed to better explain NPF in the lower troposphere, predicts unrealistically high nucleation rates over remote oceans (Lucas and Akimoto, 2006). In addition, using the activation nucleation parameterization within a box model, Chang et al. (2011) explained newly formed particles in the marine boundary layer only with elevated DMS (>100 ppt) and OH ($3*10^5$ molecules.cm^{-3}) concentrations, low background concentration and an activation coefficient lower than 10^{-7}. Nonetheless, another study performed by Yu et al. (2010) using a global model showed that activation and kinetic schemes overpredict particle number concentrations over open oceans. Although the empirical parameterizations generally tend to lead to better agreement with marine observations within specific conditions (Chang et al., 2011), the contribution of other species cannot be ruled out.

In this study, we evaluate the new empirical parameterization of nitric acid-driven nucleation quantified in Salignat et al. (accepted), building on the findings of Chamba et al. (2023). Particle concentrations simulated with the chemistry-transport model WRF-Chem (Grell et al., 2005; Fast et al., 2006) are compared against observations performed during the Sea2Cloud campaign (Sellegri et al., 2023a). In Sect. 2, instruments (Sect. 2.1) and model configuration (Sect. 2.2) are described along with the details of the implementation of the new nucleation parameterization within the model (Sect. 2.2.2). Afterwards, an overview of the nucleation events observed during the campaign is presented (Sect. 3). Finally, a comparison of modelled and observed concentrations of nanoparticles is presented together with sensitivity tests (Sect. 4).

2 Materials and methods

2.1 In situ observations over the South West Pacific

The measurements analyzed here were carried out within the framework of the Sea2Cloud project (Sellegri et al., 2023a). The campaign was conducted on board the *R/V Tangaroa* from March 17th to 27th, 2020, off the east coast of New Zealand, over the Chatham Rise, a region rarely influenced by anthropogenic emissions and mostly characteristic of open ocean conditions. A pool of instruments was deployed on the vessel, and a detailed description of the instrumental set-up involved, together with the objectives of the campaign are described in Sellegri et al. (2023a).

https://doi.org/10.5194/egusphere-2026-6891
Preprint. Discussion started: 19 November 2026
© Author(s) 2026. CC BY 4.0 License.

As this study focuses on new particle formation, we especially analyzed ambient air particles in the 1-10 nm diameter range, derived by subtracting the concentrations measured with a particle size magnifier (PSM, Air-modus A10; Vanhanen et al., 2011), which detects particles larger than 1 nm, from those measured with a condensation particle counter (CPC, TSI 3010), which detects particles larger than 10 nm. The aerosol number size distribution between roughly 10 and 500 nm was handled via a TSI scanning mobility particle sizer (SMPS) composed of a Differential Mobility Analyser (DMS) 3081, a classifier 3080 and a CPC 3772 and operated with a Kr-85 bipolar charger. Note that, in agreement with Rose et al. (2025), a correction factor of about 3.1 was applied to the SMPS concentrations (in all size bins) based on the comparison of DMPS and CPC total concentrations. In addition, a pollution filter was applied on aerosol data to avoid pollution events related to the vessel's main engine exhaust in the data analysis. This filter is based on relative wind speed and direction, along with black carbon concentrations, which were measured using a Magee Scientific Aethalometer. Meteorological parameters such as wind speed and direction, temperature, pressure, and relative humidity were measured onboard with an automated weather station (AWS) mounted on the vessel mast. Thereafter, these weather parameters were adjusted to the reference height of 10 meters above sea level using the COARE algorithm V3.6 (https://www.pmel.noaa.gov/ocs/flux-documentation, last accessed 2024/09/25). Lastly, 72-hours air mass back-trajectories of sampled air during the Sea2Cloud campaign were computed using the HYSPLIT software (Stein et al., 2015; Rolph et al., 2017), with one-hour time resolution. The segregation between the boundary layer and the free troposphere was performed following Sellegri et al. (2023a).

2.2 Model

In an effort to represent eventual nucleation events observed (Sect. 3.1) during the Sea2Cloud campaign, we used the 3-D regional chemical transport model WRF-Chem V4.1.1 (Grell et al., 2005; Fast et al., 2006). The version used here, based on the work of Marelle et al. (2017), specifically included consideration of DMS and its reactivity in the gas phase (simplified mechanism with three reactions). Following Salignat et al. (2025), we optimised the representation of aqueous DMS by using, instead of the widely used climatology of Lana et al. (2011), the aqueous DMS concentrations derived from the parameterization of Rocco et al. (2024), i.e., from nanophytoplankton cell abundances retrieved from satellite observations instead of Chl-a. Those indeed proved to better reproduce the observations of DMS over the region of interest, both in seawater and the atmosphere (Salignat et al., 2025). Furthermore, the default MOSAIC (Model for Simulating Aerosol Interactions and Chemistry, Zaveri et al., 2008) aerosol model has been revised, extended down to smaller particles in the nucleation mode using 12-bins instead of 8-bins, following the work of Lupascu et al. (2015). This 12-bins version more specifically represents particles in the model from 1 nm (instead of 39.10 nm) and up to 10 µm (see Table S1 for more details on the boundaries of each bin).

2.2.1 Atmospheric model configuration

Most of the model setup configuration has already been described in Salignat et al. (2025). The specifics of the configuration used in this work are described below. The length of the simulations in this study extends over a period of 10 days, starting

https://doi.org/10.5194/egusphere-2026-6891
Preprint. Discussion started: 19 November 2026
© Author(s) 2026. CC BY 4.0 License.

on March 13th, 2020, 12:00 UTC until March 23rd, 2020, 00:00 UTC. This period includes an extended 6-day spin-up period (ending on March 19th, 2020, 00:00 UTC), intended to allow sufficient time for the initial concentrations of nitrogen species to be flushed from the simulation's domains. The model version used here was also tuned by introducing a nitric acid-based nucleation parameterization (Salignat et al., accepted), assumed to be responsible for nighttime marine nucleation (Sect. 2.2.2), as well as sea-to-air flux of nitric oxide (NO; Sect. 2.2.2), identified as a relevant precursor to nitric acid/nitrate ions emitted by marine biota (Chamba et al., 2023; Salignat et al., accepted). Seawater emissions of isoprene and monoterpenes have also been inserted into WRF-Chem to consider their potential impact on the growth of newly formed particles (Sect. 2.2.3). The simulations were otherwise once again performed without any anthropogenic or land vegetation emissions within the simulation domain, since similar to Salignat et al. (2025), this work is primarily focusing on marine emissions (and subsequent particle formation), in view of excluding biases that could be attributable to mis-representation of these anthropogenic and vegetation sources, outside of the topic of the present paper. It has to be noted, however, that the simulations were initialized and forced at the edges of the coarser domain with concentrations supplied by the global model WACCM, which does include anthropogenic (and natural) compounds. Meteorological initial and boundary conditions were nudged with the ERA-5 reanalyzes data from the European Centre for Medium-range Weather Forecast (ECMWF, Hersbach et al., 2023a; Hersbach et al., 2023b), available at 6-hour temporal and 0.25° x 0.25° spatial resolution, and 20 vertical levels stretched between 1000 and 10 hPa. Table 1 displays the main characteristics of the WRF-Chem simulations performed in this study. Three nested domains were defined to consider impacts on a synoptic scale while also providing finer-scale results on the *R/V Tangaroa* (Fig. S1). The most resolved domain (d03), which has a spatial resolution of 3 km, is centered on the nucleation events observed in Sect. 3.1.3, aiming to evaluate the simulations against shipboard observations.

Table 1. WRF-Chem configuration

Atmospheric process	WRF-Chem option	References
Gas-phase chemistry	SAPRC-99 + DMS developments	Carter, (2000) and Marelle et al. (2017)
Aerosol model	MOSAIC 12 bins	Lupascu et al. (2015)
Photolysis	Fast J	Wild et al. (2000)
Microphysics	Morrison 2-moment scheme	Morrison et al. (2009)
Longwave radiation	Rapid Radiation Transfer Model	Mlawer et al. (1997)
Shortwave radiation	Dudhia scheme	Dudhia, (1989)
Sea salt emissions	Fuentes inorganic, high reactivity	Fuentes et al. (2011)
Cumulus parameterization	KF-CuP	Berg et al. (2015)
Planetary boundary layer	Yonsei University scheme	Hong et al. (2006)
Nucleation scheme	HNO_3 nucleation	Salignat et al. (accepted)

https://doi.org/10.5194/egusphere-2026-6891
Preprint. Discussion started: 19 November 2026
© Author(s) 2026. CC BY 4.0 License.

2.2.2 New particle formation mechanisms and precursors

The Activation and Binary nucleation schemes, which were already implemented and readily available in the standard model version, were used in this study, to allow comparison with the default configuration of WRF-Chem. The Activation mechanism is essentially a simple, empirical parameterization derived from a limited number of continental observations, where sulfuric acid (H_2SO_4) is taken as the key precursor; in this scheme, the fitted prefactor implicitly accounts for the combined effect of all other, less-characterized stabilizing vapors or environmental influences that are not treated explicitly (Semeniuk and Dastoor, 2018; Lee et al., 2019). In contrast, the Binary scheme represents the classical homogeneous nucleation involving H_2SO_4 and water (H_2O). In particular, here, the empirical Activation scheme was applied with a coefficient of $1*10^6$ particles.molecules^{-1}.s^{-1}, based on median values reported in case studies by Sihto et al. (2006), while the theoretical Binary scheme follows the formulation of Wexler et al. (1994). In addition, the parameterization linking the nucleation rate (J) to HNO_3 concentrations recently quantified (Eq. 1) by Salignat et al. (accepted) was implemented in WRF-Chem. Note that HNO_3 was used as a proxy for NO_3^- in this parameterization, since nitric acid is more widely described in atmospheric models than nitrate ions. This parameterization, which expresses a direct dependence of the nucleation rate on a single species (in our case HNO_3), was developed following the common use of power-law formulations in nucleation studies (e.g., Kulmala et al., 2006; Kuang et al., 2008; Dunne et al., 2016: Wang et al., 2022). This does not, however, rule out the contribution of other chemical species, and in particular amines, which were detected alongside nitrate ions during the measurements that led to the development of this new parameterization (Chamba et al., 2023). The involvement of amines in the process would, moreover, be in line with the current understanding, which suggests that nitric acid typically requires strong bases (e.g., DMA) to form stable clusters (Chee et al., 2019; Chen et al., 2024). It is assumed that the combined effects of environmental conditions and unidentified stabilizing species or unresolved processes, which are moreover often poorly constrained in the marine atmosphere and/or not explicitly represented in models, are reflected in the fitted parameters. In contrast with the previously mentioned mechanisms, this new empirical parameterization based on the observations of Chamba et al. (2023) and simulations performed with a multiphase chemistry box model, is specifically suited to open ocean conditions.

$$J = 3.5 * 10^{-37} * [HNO_3]^{4.807} \quad (1)$$

Where J is the nucleation rate of particles (in particles.cm^{-3}.s^{-1}) with diameter larger than 1 nm, and $[HNO_3]$ the nitric acid concentration in molecules.cm^{-3}. This parameterization was established for $[HNO_3]$ < ~2 x 10^7 molec.cm^{-3}, and its validity for higher concentrations cannot therefore be guaranteed. In this study, the simulated HNO_3 concentrations remain below this upper limit, except at higher altitudes (Sect. 3.2.3) where they can exceed it by up to one order of magnitude. Consequently, the results presented in Sect. 3.2.3 will be discussed in light of this limitation. Nevertheless, the dependence of simulated particle concentrations to HNO_3 levels in the marine boundary layer (both within and beyond the range) is analyzed in a test simulation presented in Appendix A. Please note that in the default MOSAIC version (4 or 8-bins), the Kerminen and Kulmala (2002) formula is used to handle the gap between the diameter of the freshly nucleated particles (1

https://doi.org/10.5194/egusphere-2026-6891
Preprint. Discussion started: 19 November 2026
© Author(s) 2026. CC BY 4.0 License.

nm) and the lowest size limit (39.10 nm) in the model. Using the MOSAIC version with 12-bins (with the smallest bin starting at 1 nm), the formation, growth and losses of newly formed particles are explicitly described from 1 nm.

Chamba et al. (2023) also proposed nitric oxide as the most probable seawater precursor to nitrate ions at night. The relevance of this hypothesis was verified in the modelling study of Salignat et al. (accepted), who established in addition a relationship between aqueous NO, seawater DMS concentrations and global radiation (Eq. 2). Accordingly, Eq. 2 has been introduced in WRF-Chem to provide a marine source of NO and thereby atmospheric HNO_3.

$$NO_w = \begin{cases} DMS_w * 2.5112 * 10^{-4} * \left(\frac{1+0.0659*11.22}{1+0.0659*R_g}\right), if\ DMS_w < 6.22\ nM \\ 6.22 * 2.5112 * 10^{-4} * \left(\frac{1+0.0659*11.22}{1+0.0659*R_g}\right), if\ DMS_w \geq 6.22\ nM \end{cases} \quad (2)$$

Where NO_w and DMS_w are the seawater nitric oxide and DMS concentrations in nM and R_g the global radiation in W.m^{-2}, respectively. Seawater DMS concentrations are derived from the new climatology developed by Salignat et al. (2025), based on the parameterization of Rocco et al. (2025a), which links DMS to nanophytoplankton cell abundances derived from satellite observations following Uitz et al. (2006). Please note, however, that the aqueous concentrations of NO, DMS, and then isoprene and monoterpenes (Sect. 2.2.3), implemented in WRF-Chem are not explicitly represented in seawater, as the model does not include an ocean module or aqueous-phase chemistry. Instead, these concentrations are prescribed and subsequently transferred to the gas phase using the sea-to-air exchange parametrization of Nightingale et al. (2000) (see Sect. 2.2.4).

2.2.3 Additional source of growing condensable vapor

As low and extremely low-volatility organic compounds have a significant role in the growth of newly formed particles (Kerminen et al., 2018), we also introduced new sources of biogenic VOCs in WRF-Chem. Precisely, marine isoprene and monoterpenes seawater concentrations (Eq. 3 and 4) expressed as a function of seawater DMS (like NO) (Rocco et al., 2025b) were incorporated in the model.

$$Isoprene_w[nM] = 4.70 * 10^{-2} * DMS_w[nM] \quad (3)$$

$$Monoterpenes_w[nM] = 2.42 * 10^{-2} * DMS_w[nM] \quad (4)$$

In the version of the model employed in this study, the condensation of organic species, including oxidation products of isoprene and monoterpenes, is accounted following the simplified volatility basis-set two-dimensional (VBS) approach (Shrivastava et al., 2011). This approach specifically clusters organic gaseous species into different volatility classes (logarithmically separated by saturation concentrations sections C* of the compounds) accounting for hygroscopicity and ageing of organic vapors by oxidation. By default, our model version groups biogenic compounds in only 1 section, with a C* value set at 1 µg.m^{-3}. Following the recommendation of Lupascu et al. (2015), the volatility of biogenic species has been reduced to 10^{-3} µg.m^{-3}, to promote condensation from 1 nm particles (instead of around 30 nm).

https://doi.org/10.5194/egusphere-2026-6891
Preprint. Discussion started: 19 November 2026
© Author(s) 2026. CC BY 4.0 License.

2.2.4 Sea-to-air transfer of injected seawater species

Nitric oxide, along with isoprene and monoterpenes, are then transferred from the aqueous phase towards the gaseous phase to react with the other compounds and produce the compounds of interest (HNO_3 and biogenic species). In this regard, we proceed in the same way as for DMS (Salignat et al., 2025), i.e., following the Marelle et al. (2017) procedure involving the Nightingale et al. (2000) transfer velocity parameterization. However, unlike DMS, for which atmospheric concentrations were neglected in the transfer equation (flux supposed unidirectional), the sea-to-air transfer scheme (F, in mol.m^{-2}.s^{-1}) employed for these three new species is calculated as in Tian et al. (2020), using the relation of McGillis et al. (2002) (Eq. 5). This parameterization is bidirectional and considered better suited for more reactive species.

$$F = K_w * (C_w - P_p * H) \quad (5)$$

Where K_w is the transfer velocity (in cm.hr^{-1}), computed using the coefficients from Nightingale et al. (2000), C_w the seawater nitric oxide/isoprene/monoterpenes concentrations in nM, P_p the partial pressure of the species in air (in atm), which is directly related to their atmospheric concentrations, and H the Henry law constant. The Henry's law constant was computed following the temperature-dependent formulation of Sander et al. (2023), where the values of H_0 (Henry's law constant at the reference temperature) and B (the temperature dependent parameter) taken from Sander et al. (2023) were respectively $H_0 = 1.9*10^{-5}$ mol.m^{-3}.Pa^{-1}, B = 1790 K, $H_0 = 3.4*10^{-4}$ mol.m^{-3}.Pa^{-1}, B = 4400 K, and $H_0 = 2.9*10^{-4}$ mol.m^{-3}.Pa^{-1}, B = 1800 K, for NO, isoprene, and monoterpenes.

In absence of relevant literature, the Schmidt number for NO used in the Nightingale et al. (2000) relation (not shown here) was computed as the ratio of the kinematic viscosity, estimated according to the Andreas (2005) relation, and the molecular diffusivity, calculated in line with Wise and Houghton (1968) parameterization. The Schmidt numbers of isoprene and monoterpenes have been approximated using the same relationships proposed by Palmer and Shaw (2005), i.e., as a function of surface seawater temperature.

https://doi.org/10.5194/egusphere-2026-6891
Preprint. Discussion started: 19 November 2026
© Author(s) 2026. CC BY 4.0 License.

3 Results

3.1 Observation and analysis of new particle formation events

3.1.1 Overview of meteorological conditions during the Sea2Cloud campaign

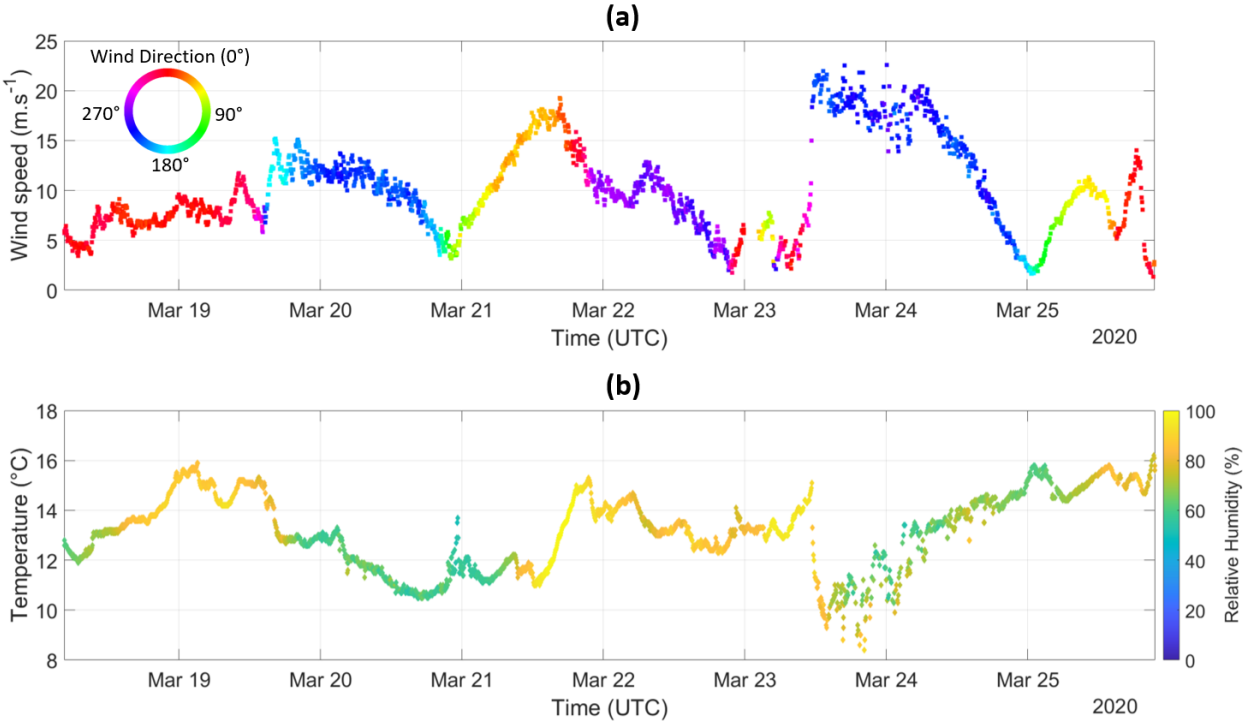


Figure 1: Overview of the meteorological conditions during the Sea2Cloud campaign (March 2020) with time series of (a) measured wind speed and direction, and (b) measured temperature and relative humidity.

A detailed description of the measurements and meteorological conditions during the Sea2Cloud campaign is provided in Sellegri et al. (2023a). Figure 1 describes the temporal evolution of wind speed and direction (Fig. 1.a), along with air temperature and relative humidity (Fig. 1.b), as measured onboard the *R/V Tangaroa*. In brief, the sampled air masses were predominantly of marine origin, with wind directions mainly from the southwest, i.e., from the Southern Ocean. Nevertheless, some terrestrial and/or anthropogenic influence cannot be excluded when the wind originates from the north or west, potentially bringing air from New Zealand. Based on the analysis of 72-hour backward trajectories presented in Sellegri et al. (2023a), 54% of the sampled air masses crossed over New Zealand during the period from March 19-25, 2020, yet in this case they (1) spent on average only approximately 11% of their time (about 8 hours in general) within New Zealand's continental boundary layer, and (2) spent at most 50 continuous hours (on average 17 hours) in the marine boundary layer after their last contact with land before sampling. This suggests that, overall, the campaign captured mostly pristine marine conditions. Figure 1.a further depicts that wind speeds averaged around 10 $m.s^{-1}$, with peaks reaching up to 23 $m.s^{-1}$ on March 23, 2020, UTC. Such high wind speeds could inhibit new particle formation by enhancing sea spray

https://doi.org/10.5194/egusphere-2026-6891
Preprint. Discussion started: 19 November 2026
© Author(s) 2026. CC BY 4.0 License.

formation, which increases the condensation sink. During the same period, air temperature ranged between 8.4 and 16.2 °C, and relative humidity varied from 50 to 99 % (Fig. 1.b). Within these ranges, temperature and relative humidity are not expected to strongly influence nucleation rates.

3.1.2 Analysis of the aerosol size distribution

Although measurements during the Sea2Cloud campaign were predominantly conducted in marine air masses (Sellegri et al., 2023a), as discussed above, some sampled air masses had spent time over land (particularly over New Zealand) in the 72 hours preceding measurement. This terrestrial influence could bias the representativeness of the aerosol size distributions for a truly marine environment. To overcome this, we applied a strict filtering criterion, selecting only those air masses that spent at least 90% of the last 72 hours over the ocean. This filter limits terrestrial influence to a maximum of 7 hours, and allows for the generation of median particle spectra that more faithfully represent pristine marine conditions while still retaining sufficient data.

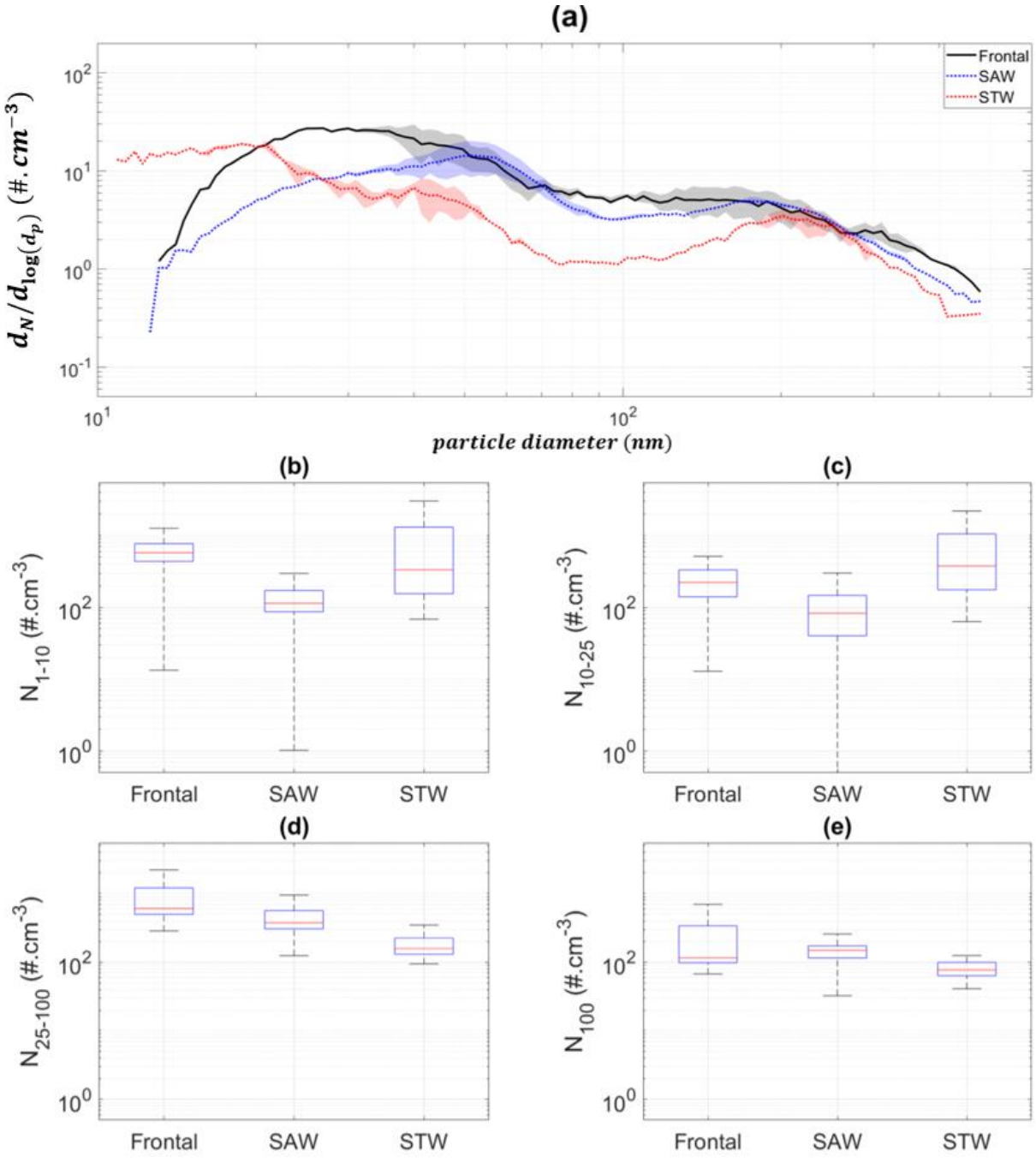
On its voyage, the *R/V Tangaroa* received air masses that had flew over various seawater masses with differing biomass concentrations *(Sellegri et al. 2023a)*, ranging from high in frontal seawater (March 17-20, 2020), to low in sub-Antarctic seawater (March 20-23, 2020), and intermediate in subtropical seawater (March 24-25, 2020). Since marine biology is suspected to influence pristine oceanic new particle formation, the aerosol size distributions observed during the campaign are expected to reflect the overflew seawater type.

Figure 2.a shows the median aerosol size distributions observed during the Sea2Cloud campaign (March 19-25, 2020) under these filtered conditions for each seawater type encountered. To quantify variations in particle size distributions, we also present boxplots (Fig. 2.b-e) of integrated number concentrations in the nucleation (10-25 nm), Aitken (25-100 nm), and accumulation (>100 nm) modes, as well as in the sub-10 nm range (1-10 nm) using PSM data. Overall, median size distributions are characterized by features consistent with marine air masses, typically featuring a trimodal pattern dominated by an Aitken mode and flanked by nucleation and accumulation modes, consistent with previous observations (Sellegri et al., 2023a). The size distributions over frontal and sub-Antarctic seawater are similar for particles larger than 50 nm. However, the low biomass conditions in sub-Antarctic seawater strongly impact particle concentrations in the smaller size ranges: the nucleation mode is absent, and the distribution is dominated by Aitken and accumulation modes. As a result, air masses sampled over sub-Antarctic seawater exhibit the lowest concentrations in the $N_{1\text{-}10}$ and $N_{10\text{-}25}$ ranges, with median values (25^{th}-75^{th} percentiles) of 113 (87-171) and 83 (40-147) particles.cm^{-3}, respectively (Fig. 2.b-d). Conversely, air masses sampled in frontal and subtropical seawater show a clear nucleation mode and elevated particle concentrations, suggesting a biological contribution to new particle formation. Median $N_{1\text{-}10}$ concentrations (25^{th}-75^{th} percentiles) reach 574 (436-768) and 333 (155-1306) particles.cm^{-3} over frontal and subtropical seawater, respectively (Fig. 2.b), with $N_{10\text{-}25}$ concentrations striking 223 (140-332) and 378 (176-1053) particles.cm^{-3}, respectively (Fig. 2.c). In the end, for the three seawater types, particle number concentrations within the Accumulation mode are all reduced compared to smaller diameters, with median

https://doi.org/10.5194/egusphere-2026-6891
Preprint. Discussion started: 19 November 2026
© Author(s) 2026. CC BY 4.0 License.

concentrations (25^{th}-75^{th} percentiles) of 116 (98-339), 149 (115-173), and 77 (64-99) particles.cm^{-3} for frontal, sub-Antarctic, and subtropical seawater respectively, consistent with values reported in the subtropical Pacific Ocean (Ueda et al. 2016). These aerosol size distributions and concentration levels are comparable to those reported for summer marine air masses at Baring Head, New Zealand (Peltola et al., 2022) or Mace Head, Ireland (Yoon et al., 2007). Separate day/night analyses of particle size distributions revealed no significant differences (Fig. S2), suggesting that solar radiation does not strongly impact the marine aerosol size distributions sampled during the campaign. This lack of diurnal variation likely reflects the long atmospheric residence times of sampled particles, which smooth out short-term influences through ageing, condensation, and mixing during transport.

https://doi.org/10.5194/egusphere-2026-6891
Preprint. Discussion started: 19 November 2026
© Author(s) 2026. CC BY 4.0 License.



290 **Figure 2: (a) Median aerosol size distribution measured with the SMPS in clean ambient marine air masses during the Sea2Cloud campaign, classified according to seawater types crossed by the *R/V Tangaroa*: frontal (Frontal), sub-Antarctic (SAW) or sub-tropical (STW) seawaters. Air masses were filtered based on 72-hour backwards trajectories (≥ 90% time over ocean) and on the pollution filter described in Sect. 2.1. Boxplots show particle number concentrations associated with the different water masses for the size ranges (b) $N_{1\text{-}10}$, (c) $N_{10\text{-}25}$, (d) $N_{25\text{-}100}$ and (e) N_{100}. In each boxplot, the central line indicates the median, the bottom and top**

https://doi.org/10.5194/egusphere-2026-6891
Preprint. Discussion started: 19 November 2026
© Author(s) 2026. CC BY 4.0 License.

edges correspond to the 25th and 75th percentiles, respectively, and the whiskers extend to the most extreme data points excluding outliers.

3.1.3 Detection and characterization of nucleation events

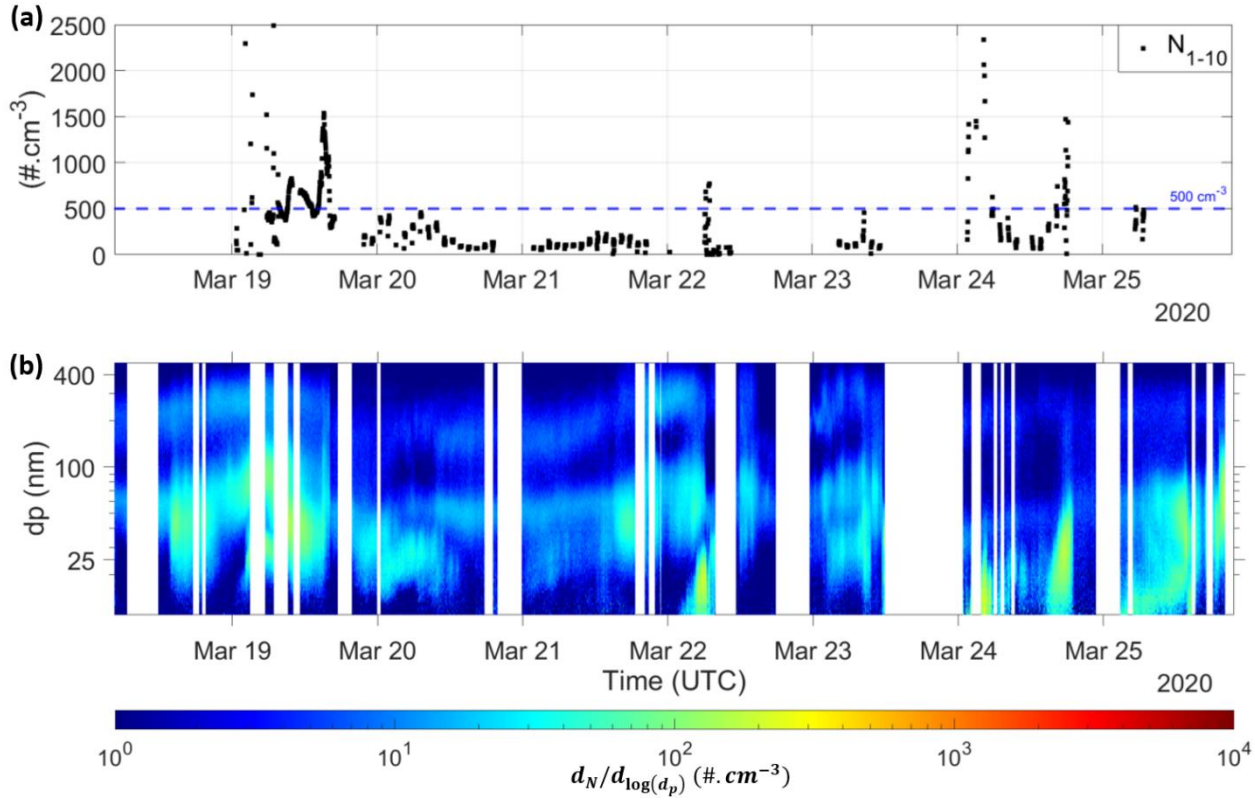


Figure 3: (a) Time series of sub-10 nm particle concentrations ($N_{1\text{-}10}$) measured with a PSM during the Sea2Cloud campaign. The dotted blue line represents the threshold above which an increase in $N_{1\text{-}10}$ concentrations can be considered indicative of a NPF event, as proposed by Peltola et al. (2022). (b) Aerosol size distribution measured with a SMPS in the framework of the Sea2Cloud campaign. Both panels are shown in UTC time. Blank gaps in both panels correspond to periods flagged as polluted and removed using the pollution filter described in Sect. 2.1.

A new method for detecting new particle formation events, specifically suited to remote marine atmospheres, was recently proposed by Peltola et al. (2022). Unlike the classical criteria established by Dal Maso et al. (2005) for continental NPF events (which rely on the visual analysis of the temporal evolution of particle size distributions measured with a SMPS), this new approach identifies marine NPF events using a threshold based on sub-10 nm particles concentrations. The classical criterion is indeed challenging to apply in the marine boundary layer, as it rarely identifies NPF events in pristine marine air masses (Peltola et al., 2022). Additionally, the SMPS instrument may underestimate particle number concentration in the 10-15 nm range due to particle losses in sampling lines (Wiedensohler et al., 2012), which is particularly problematic for nascent clusters at low concentrations. Furthermore, particle growth in the marine atmosphere is ordinarily slow and can extend over more than one day (O'Dowd et al., 2010, Peltola et al., 2022), making it more difficult to identify the

https://doi.org/10.5194/egusphere-2026-6891
Preprint. Discussion started: 19 November 2026
© Author(s) 2026. CC BY 4.0 License.

characteristic shapes of NPF events classically performed on a daily basis. Given that nucleation and subsequent particle growth are frequent in marine air masses (Peltola, 2021) and are often governed by different processes compared to continental NPF, this new approach defines a NPF event when the particle number concentration in the 1-10 nm size range exceeds 500 particles.cm^{-3}.

Figure 3.a presents the time series of $N_{1\text{-}10}$ nm particles measured with a PSM during the Sea2Cloud campaign. Applying the marine-specific criterion proposed by Peltola et al. (2022), four NPF events were identified throughout the campaign, on March 19 (nighttime, 09:00 – 16:00 UTC), 22 (late evening, 06:00 – 07:00 UTC), and 24 (afternoon and early morning, 01:00 – 06:00 & 16:00 – 19:00 UTC), 2020, with two distinct events potentially occurring on March 24. For these events, continued particle growth into larger sizes can be observed in Fig. 3.b.

Nevertheless, the two NPF events observed on March 24 are potentially not representative of pristine marine air mass conditions. As illustrated in Fig. S3.c-d, the air sampled aboard the *R/V Tangaroa* on that day spent at most 11 hours within the marine boundary layer and followed a trajectory along the eastern coast of New Zealand's South Island, passing over urban areas such as Christchurch and, earlier, Queenstown. This extended passage through the continental boundary layer likely introduced non-marine precursors, suggesting that these events were influenced by anthropogenic or terrestrial sources. As a result, we excluded the March 24 events from our analysis. In contrast, the NPF event on March 22 was sampled under significantly different conditions. According to Fig. S3.b, the corresponding air masses spent between 12 and 24 continuous hours within the marine boundary layer over Chatham Rise prior to sampling. It is therefore plausible that these air masses were enriched with biogenic precursors emitted by the Chatham Rise marine ecosystem, and hence with a marine signature, resulting in a marine nucleation. However, we cannot exclude an anthropogenic influence, since air masses travelled over Christchurch (25 hours before sampling) and Wellington (36 hours prior to sampling). Similarly, the NPF event observed on March 19 (characterized by two bursts) occurred while air masses had resided for 14 to 18 hours within the marine boundary layer (Fig. S3.a). Although the trajectory originated from the Cook Strait (with a potential anthropogenic signature), the air spent up to 12 hours above the Chatham Rise, likely accumulating marine biogenic precursors. Consequently, based on air mass origin and particle number characteristics ($N_{1\text{-}10}$), we consider the nucleation events on March 19 and 22, 2020, to be representative of marine new particle formation. Both events occurred at night, under conditions of low UVa radiation. During these two NPF events, the median wind speed was 10.4 m.s^{-1} (inter-quartile range: 8.1-11.1 m.s^{-1}), the air temperature was 14.2°C (13.9-14.6°C), and the relative humidity was 80% (78.1-82.7%). In both cases, air masses remained predominantly within the marine boundary layer prior to sampling (Fig. S3).

3.2 Simulation of new particle formation events using WRF-Chem

This section aims to evaluate whether the two NPF events identified in Sect. 3.1.3 can be represented using the WRF-Chem model (Sect. 2.2). As previously mentioned, WRF-Chem already includes several nucleation parameterizations (Sect. 2.2.2) which will first be tested and assessed in Sect. 3.2.1 (simulations *Activation* and *Binary*, see Table 2). These are then compared in Sect. 3.2.2 with the newly implemented nucleation scheme detailed in Sect. 2.2.2 (simulation *HNO_3 nucleation*,

https://doi.org/10.5194/egusphere-2026-6891
Preprint. Discussion started: 19 November 2026
© Author(s) 2026. CC BY 4.0 License.

Table 2). It should be noted that the three simulations mentioned above include marine isoprene and monoterpenes fluxes as described by Eq. (3) and (4). In order to highlight the role of the oxidation products of these compounds in the growth and survival of nucleated particles, a simulation in which their fluxes were cut off was also performed (*HNO_3 nucleation Ø BVOC fluxes*). All these simulations aim to evaluate the performance of existing and new nucleation mechanisms in simulating the occurrence of NPF in the remote marine boundary layer. To this end, simulated concentrations of ultra-fine particles (1-10 nm diameter) will be compared with those observed along the *R/V Tangaroa* trajectory during the Sea2Cloud campaign. All simulations include marine fluxes of isoprene and monoterpenes and are revised to promote particle growth from 1 nm (see Sect. 2.2.3), while an additional simulation is run without marine BVOC fluxes to specifically assess their potential role in NPF. An overview of the different simulations performed in this study is given in Table 2.

Table 2. Overview of the different nucleation simulations performed in the present work.

WRF-Chem simulation name	Nucleation parameterization used	References
Activation	Activation-type ($J = 2 \times 10^{-6} \times [H_2SO_4]$)	Wang and Penner (2009)
Binary	Binary (H_2SO_4-H_2O)	Wexler et al. (1994)
HNO_3 nucleation	$J = 3.5 \times 10^{-37} \times [HNO_3]^{4.807}$	Salignat et al. (accepted)
HNO_3 nucleation Ø BVOC fluxes	$J = 3.5 \times 10^{-37} \times [HNO_3]^{4.807}$	Salignat et al. (accepted)
HNO_3 nucleation Ø marine NO fluxes	$J = 3.5 \times 10^{-37} \times [HNO_3]^{4.807}$	Salignat et al. (accepted)

3.2.1 Simulation with established nucleation mechanisms

To begin with, we attempted to reproduce the particle number concentrations observed throughout the Sea2Cloud campaign, particularly the two nocturnal NPF events described in Sect. 3.1.3, using the default nucleation mechanisms available in WRF-Chem (Sect. 2.2.2). Figure 4 presents both observed and simulated hourly mean number concentrations of newly formed particles in the 1-10 nm diameter range, obtained from the Activation (Fig. 4.a) and Binary (Fig. 4.b) nucleation schemes, both of which rely on H_2SO_4 concentrations.

As shown in Fig. 4.a (please note the different scales of the right and left axis), the Activation scheme significantly overestimates particle number concentrations during the day, with simulated values exceeding observations by roughly an order of magnitude on average (RMSE = 5185 particles.cm^{-3}, Spearman's ρ = -0.04, p-value = 0.74). Simulations' peaks reached up to 20420 particles.cm^{-3}, resulting in a substantial mean overestimation of 2636 particles.cm^{-3} compared to Sea2Cloud observations. This overprediction is potentially due to the fact that the empirical nucleation parameterization used in the Activation scheme is based on measurements from continental environments (Kulmala et al., 2006; Sihto et al., 2006; Riipinen et al., 2007) or in simulation chambers (Sipilä et al., 2010; Kirkby et al., 2011; Almeida et al., 2013), raising questions about the central role of sulfuric acid in nucleation. In addition, the empirical factor underlying the Activation scheme (here $2*10^{-6}$ particles.molecules^{-1}.s^{-1}) varies considerably across environments (Sihto et al., 2006; Kuang et al., 2008; Spracklen et al., 2010), suggesting that nucleation is influenced by possibly environment-dependent species beyond sulfuric

https://doi.org/10.5194/egusphere-2026-6891
Preprint. Discussion started: 19 November 2026
© Author(s) 2026. CC BY 4.0 License.

acid (Jokinen et al., 2018; Brean et al., 2021; Peltola et al., 2023; Chamba et al., 2023). These discrepancies likely explain the unrealistically high particle formation rates in the model. Additionally, the Activation mechanism appears unsuitable for simulating nocturnal NPF in the remote marine atmosphere, as it primarily triggers nucleation during daylight hours (Fig. 4.a).

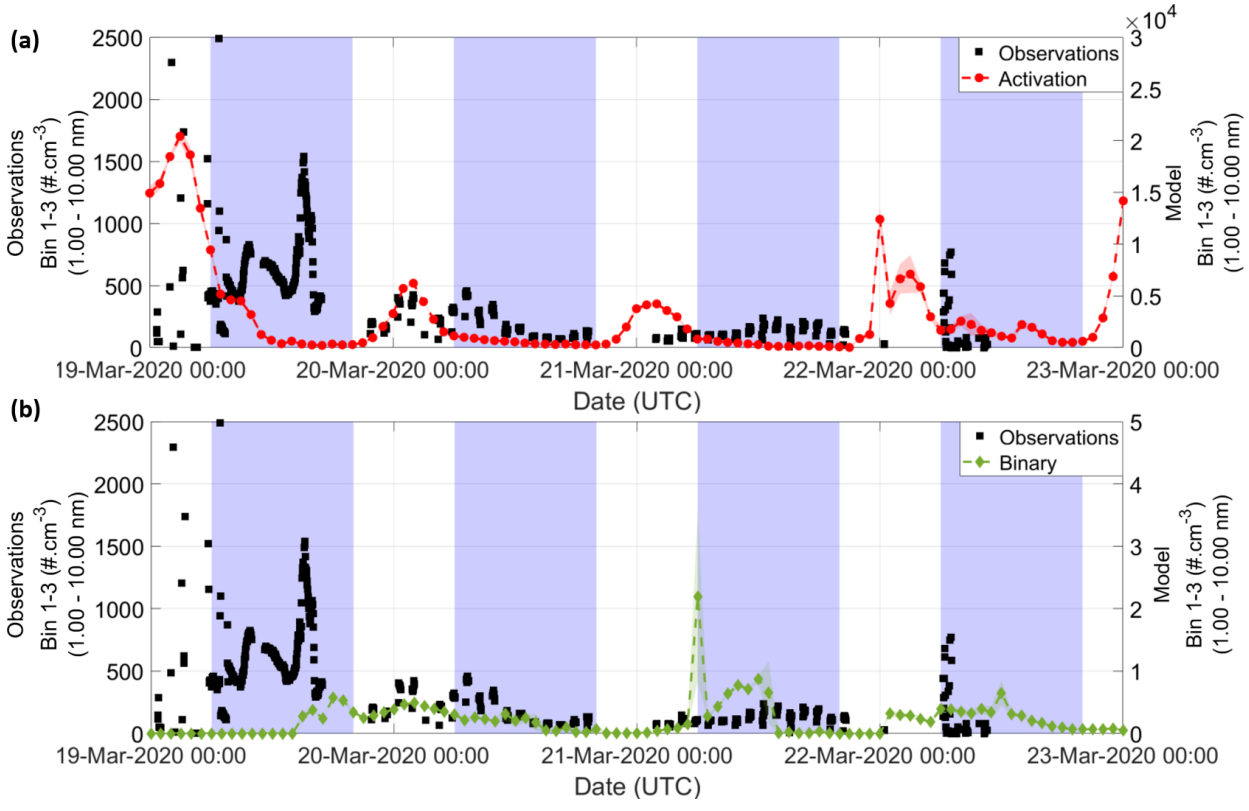


Figure 4: Time series of discrete observations (left-axis) and simulated hourly (right-axis) particle number concentrations between 1 and 10 nm using the (a) *Activation* and (b) *Binary* nucleation mechanisms available by default in the WRF-Chem model. Blue patches depict nighttime periods, and shaded boundaries around modelled concentrations represent their standard deviation along the ship's path. Note that the scales vary depending on the axis.

On the other hand, the Binary nucleation scheme produces only very low particle number concentrations in the marine boundary layer, with values dropping to as little as 2.2 particles.cm^{-3}, resulting in an underestimation by approximately three orders of magnitude (RMSE = 411 particles.cm^{-3}, Spearman's ρ = -0.28, p-value = 0.02) compared to the observations (Fig. 4.b). This limitation has already been observed in the boundary layer by Lucas and Akimoto (2006) using the binary nucleation scheme of Vehkamäki et al. (2002) in a global atmospheric model. Although the modelled particle number concentrations using the Binary scheme appear to slightly increase at night, no effective nucleation takes place under our simulation conditions with this scheme. This highlights the difficulty of representing marine boundary layer nucleation using the binary scheme currently implemented in WRF-Chem. It is worth noting, however, that this scheme is relatively outdated. Recent developments, such as the updated Binary nucleation parameterization proposed by Määttänen et al. (2018) based on

https://doi.org/10.5194/egusphere-2026-6891
Preprint. Discussion started: 19 November 2026
© Author(s) 2026. CC BY 4.0 License.

simulation chamber experiments, aim to improve the realism and applicability of this mechanism, particularly under marine conditions, and may offer a promising alternative for future model developments.

Ultimately, this figure highlights that the Activation and Binary nucleation mechanisms, commonly used and implemented by default in atmospheric models, fail to reproduce the occurrence of nocturnal NPF events in the pristine marine atmosphere. The Binary scheme, in particular, may be more relevant in the cold upper troposphere (Dunne et al., 2016). These findings emphasize the need to either adapt existing nucleation mechanisms or implement new parameterizations specifically tailored to capture NPF processes in the nocturnal pristine marine boundary layer.

3.2.2 Simulation of $N_{1\text{-}10}$ with the new nitric acid-based nucleation mechanism

As presented in Sect. 2.2.2, Chamba et al. (2023) revealed the evidence of nighttime atmospheric nucleation driven by nitrate ions (NO_3^-) in a natural pristine marine environment. Building on these findings, a new nucleation parameterization based on HNO_3 concentrations has recently been quantified (Salignat et al., accepted, Eq. 1). This mechanism was implemented in WRF-Chem alongside a DMS-dependent nocturnal NO source (Salignat et al., accepted, Eq. 2) designed to reproduce nighttime HNO_3 production from marine biological activity.

Figure 5.a illustrates Sea2Cloud observations alongside simulated hourly mean number concentrations of newly formed particles in the 1-10 nm size range, using the HNO_3-based nucleation scheme (Sect. 2.2.2). This parameterization more accurately captures the observed levels of ultrafine particle concentrations (RMSE = 332 particles.cm^{-3}, Spearman's ρ = 0.40, p-value = 5.35*10^{-4}), producing values of the same order of magnitude as the observations, unlike the default activation and binary schemes (Sect. 3.2.1). In particular, the temporal variability of the first nocturnal NPF event (March 19, 2020) observed during the campaign (Sect. 3.1.3) is well reproduced (Spearman's ρ = 0.54; p-value = 0.06), with simulated concentrations closely matching observations, although with a slight underestimation (mean bias = -17 particles.cm^{-3}). This result suggests that, although the air masses associated with this event originated from the Cook Strait and could have been influenced by anthropogenic emissions (not included in the simulations), such influence likely played only a minor role. Instead, recent or local marine biological activity appears to have been the primary driver of the NPF event observed on March 19, 2020. In contrast, the second NPF event observed on March 22, 2020, is entirely missed by the model. This may indicate that nucleation was driven by nucleating species other than HNO_3, and/or implied a mechanism not yet represented in WRF-Chem, or alternatively, an anthropogenic signature in the measurement that was not accounted for in the simulations. In fact, while this event was classified as marine (Fig. S3.b), we cannot exclude that the air mass in which it was observed may have retained some continental influences after passing over urban areas in New Zealand, or may have been enriched in ship-derived precursors (Sect. 3.1.3), which are not represented in the simulations.

Furthermore, on March 20 and 21, when air masses were exclusively of pristine Southern Ocean origin, the model failed to simulate any $N_{1\text{-}10}$ particles. While no NPF events were formally identified during this period (Sect. 3.1.3), observations still show the presence of ultrafine particles. This difference could be linked to a limitation in the representation of sea spray aerosols (SSA) number fluxes in the model, since 1) wind speeds on the 20th and 21st were higher than at the beginning of the

https://doi.org/10.5194/egusphere-2026-6891
Preprint. Discussion started: 19 November 2026
© Author(s) 2026. CC BY 4.0 License.

period, which could have favored the emission of SSA, and 2) nanoparticles emissions from bubble bursting were on the other hand evidenced in nascent sea spray experiments (Fuentes et al., 2010; Schwier et al., 2015; 2017), especially in cold waters (Sellegri et al., 2023b). In this work, sea spray emissions were considered in all particle size bins, but with the default model configuration, in which the impact of marine biology on the associated number fluxes is underestimated (Sellegri et al. 2021, 2023b; Rose et al., 2025). While the role of marine microorganisms was in particular shown to be crucial in predicting primary CCN-sized particle concentrations (Rose et al., 2025), its impact on predicting < 10 nm particle concentrations will however require further study, due to expected interference with nucleation occurrence (in relation to condensation sink variations).

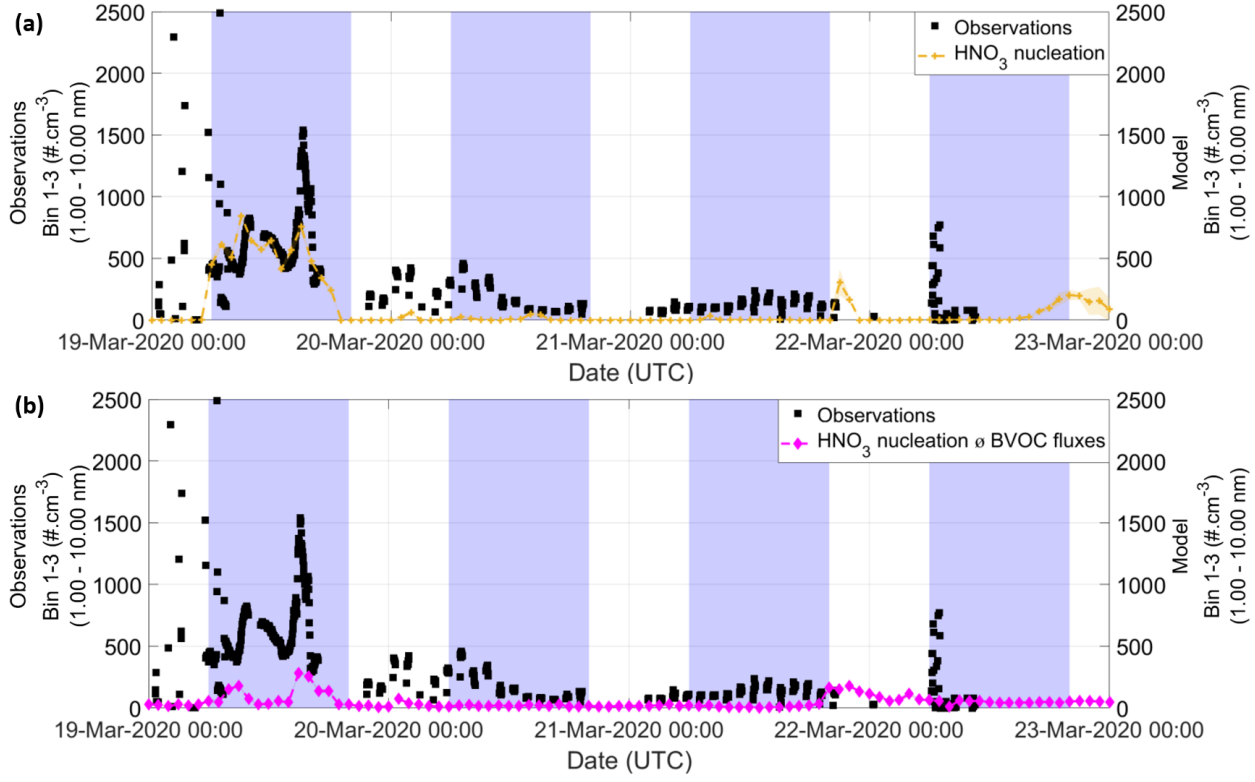


Figure 5: Time series of discrete observations (left-axis) and simulated hourly (right-axis) particle number concentrations using the new nitric acid nucleation mechanism presented in Salignat et al. (accepted) with (a) or without (b) seawater biogenic volatile organic compounds emissions (isoprene and monoterpenes). Blue patches depict nighttime periods, and shaded boundaries around modelled concentrations represent their standard deviation along the ship's path.

Given the suspected role in new particle formation of the marine species fluxes (Eq. 2, 3, and 4) implemented in our model configuration, alongside the nucleation parameterization, we examine now how these marine fluxes impact the concentrations of key compounds in our simulations.

In particular, to further assess the role of marine biogenic VOCs on modelled $N_{1\text{-}10}$ particle concentrations, we conducted a sensitivity simulation in which the biogenic emissions fluxes of isoprene and monoterpenes were excluded. As illustrated in

https://doi.org/10.5194/egusphere-2026-6891
Preprint. Discussion started: 19 November 2026
© Author(s) 2026. CC BY 4.0 License.

Fig. 5.b, the absence of seawater BVOCs emissions results in a significant decrease in $N_{1\text{-}10}$, likely reflecting a strong impact on the survival and growth of the newly formed particles in the marine atmosphere. While the HNO_3-based nucleation scheme still performs better than the default nucleation schemes when BVOC fluxes are excluded (RMSE = 384 particles.cm^{-3}, Spearman's ρ = 0.06, *p*-value = 0.60), it nonetheless underestimates the observed concentrations in the 1-10 nm size range. This highlights the critical role of biogenic compounds in enabling the growth and persistence of ultrafine particles in remote oceanic environments, and, more broadly, the importance of adequately representing both nucleation and particle growth.

Finally, to investigate the role of including a marine source of NO (Eq. 2) in our simulations, and more specifically its impacts on HNO_3 concentrations and, consequently, on new particle number concentrations ($N_{1\text{-}10}$), we analyzed the time series of these two variables for two set of simulations: *HNO_3 nucleation* and *HNO_3 nucleation Ø marine NO fluxes* (Fig. S5). Figure S5 shows that the impact of the marine NO source is surprisingly small on both 1) HNO_3 concentrations (Fig. S5.a) and 2) $N_{1\text{-}10}$ particle number concentrations (Fig. S5.b) with median ratios of 1.01 and 1.4 respectively. Hence, the addition of a marine source of NO (Eq.2) plays a minor role in new particle formation compared to the nucleation parameterization itself (Eq. 1). Note that although simulated HNO_3 concentrations remain relatively low (~9*10^6 molec.cm^{-3}), our empirical parameterization likely captures the influence of additional environmental and chemical factors through its fitted coefficients, resulting in nucleation despite depleted HNO_3 concentrations. Yet, we stress here that our marine biogenic NO source may be underestimated. First, Eq. 2 was parameterized using simulated seawater NO concentrations at the lower end of measured values (Salignat et al., accepted), which are themselves approximately three orders of magnitude lower than those reported by Arkian et al. (2025). Second, a potentially large NO source may arise from photochemical processes, an unrepresented process in WRF-Chem, which could substantially enhance the marine NO_x reservoir, as pointed by Arkian et al. (2025). Further work is therefore needed, including improved characterization of marine NO sources and a better understanding of the underlying processes.

In the end, the HNO_3-based nucleation parameterization, together with the addition of marine BVOC fluxes, significantly improve the ability of the model to reproduce the nocturnal NPF event observed on March 19th. Yet, the relevance of this new mechanism to other marine environments remains uncertain. Indeed, the sensitivity of this mechanism to local nitric acid concentrations and biological precursors suggests that its performance may vary across different oceanic regions. In addition, the validity of the parameterizations used to express the fluxes of the compounds of interest (Eq. 2, 3, 4) is not guaranteed outside the geographical area of this study. Consequently, this case study should be viewed as an initial step toward assessing the role of nitrate-driven nucleation in the marine atmosphere, with a broader validation needed under diverse marine conditions.

3.2.3 Preliminary assessment of new particle formation in the upper atmosphere

Although this study focuses specifically on the marine boundary layer, where the Sea2Cloud observations were conducted, and for which associated parameterizations (nucleation and precursor fluxes) were in turn developed, we also start to explore

https://doi.org/10.5194/egusphere-2026-6891
Preprint. Discussion started: 19 November 2026
© Author(s) 2026. CC BY 4.0 License.

the potential impact of these new boundary layer sources in the upper atmosphere (without additional model development or additional sources of HNO_3 specific to these altitudes). In particular, NPF is assumed to be favored in the marine free troposphere, where newly formed particles can subsequently be entrained downward into the marine boundary layer. Therefore, the impacts on the new mechanism and new marine precursor fluxes in the upper atmosphere would only reflect the upward transport of marine boundary layer species rather than contributions from in-situ high-altitude sources. Note that the results discussed in this section remain preliminary, as no observations were available at such altitudes during the Sea2Cloud campaign.

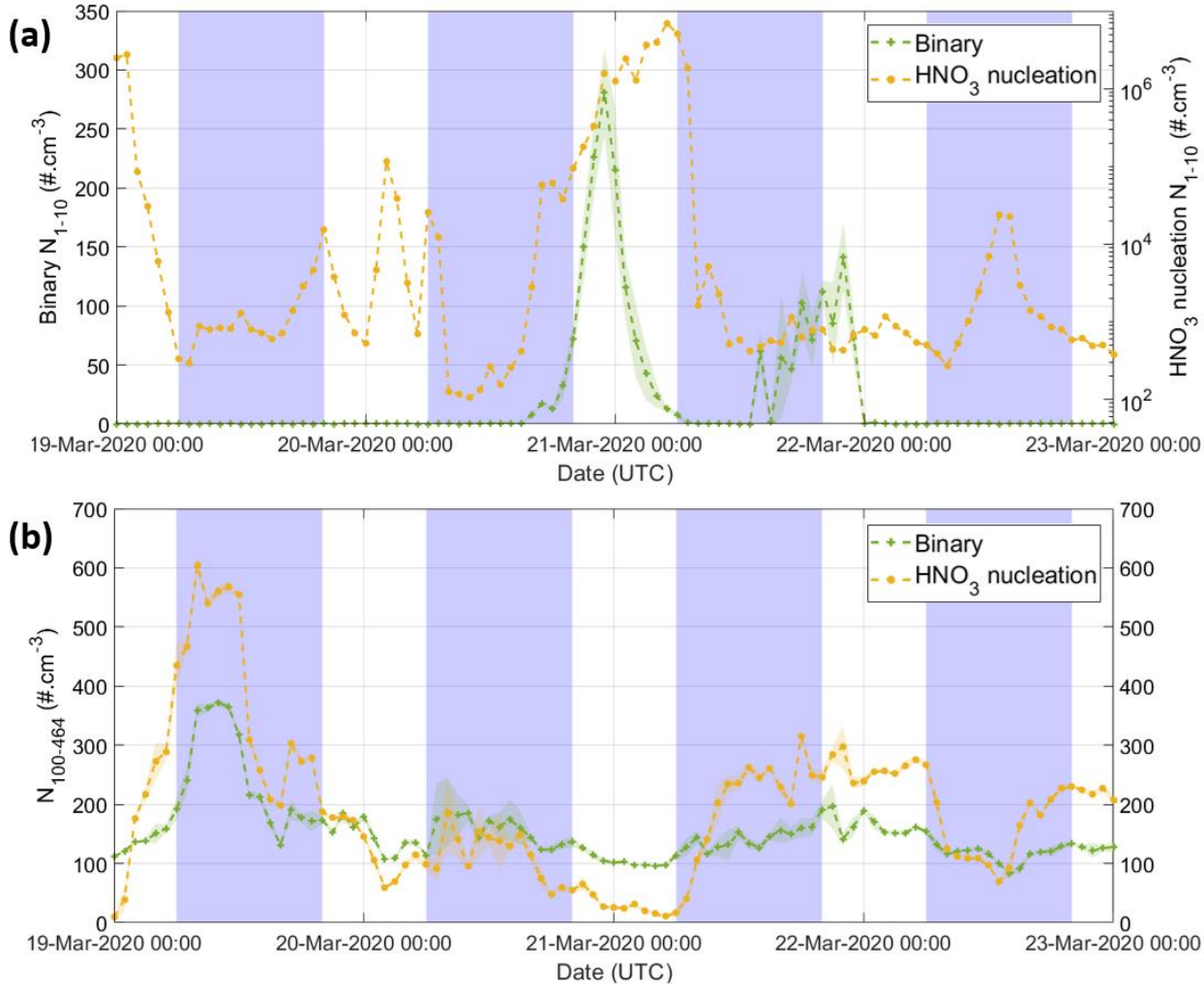


Figure 6: Time series of simulated (a) $N_{1\text{-}10}$ and (b) $N_{100\text{-}464}$ hourly particle number concentrations using the new nitric acid-based nucleation mechanism and the binary scheme at 850 hPa. Blue patches depict nighttime periods, and shaded boundaries around modeled concentrations represent their standard deviation along the ship's path. Note that the scales vary depending on the axis on the panel (a).

https://doi.org/10.5194/egusphere-2026-6891
Preprint. Discussion started: 19 November 2026
© Author(s) 2026. CC BY 4.0 License.

Figure 6.a shows the temporal evolution of simulated $N_{1\text{-}10}$ particle number concentrations at 850 hPa, an altitude relevant to cloud formation, along the *R/V Tangaroa*'s trajectory, using both the classical binary nucleation scheme and the new nitric acid-based nucleation parameterization. It is important to note that the y-axis differs between the two simulations due to large differences in magnitude. As observed at sea level (Sect. 3.2.2), the new parameterization produces significantly higher particle number concentrations, up to 8 orders of magnitude, compared to the binary scheme. Although the binary scheme is supposed to appear more relevant to the colder conditions of the upper troposphere (Spracklen et al., 2005; Dunne et al., 2016), it yields only a median concentration of 4.8 * 10^{-3} particles.cm^{-3} at 850 hPa, but occasionally leads to early morning spikes up to 300 particles.cm^{-3}. These episodic increases are more consistent with the concentration levels modeled by Dunne et al. (2016) using a binary mechanism. In contrast, the new nitric acid-based scheme yields much higher particle concentrations, as simulated at sea level (Sect. 3.2.2), with a median of 878 particles.cm^{-3} and daytime peaks reaching as high as 1.5 * 10^{6} particles.cm^{-3}, which are even higher that those simulated at low altitude, likely driven by greater availability of nitric acid at these high altitudes. These elevated daytime values in the simulations are driven by nitric acid concentrations peaks (increasing by a factor of ≈ 14 compared to simulated median concentrations) which deserve additional or deeper investigation. There are very few high-altitude measurements to compare with, particularly over the ocean. Yet, the modeled concentrations resulting from the nitric acid-based nucleation appear on average closer to the observations performed at the high-altitude puy de Dôme observatory (1465 m a.s.l) (Rose et al., 2015) than those resulting from the binary mechanism. Indeed, concentrations in the range between 10^{2} and 10^{4} particles.cm^{-3} were observed at puy de Dôme for 1-2.5 nm diameter particles in the interface layer between the boundary layer and the free troposphere.

In contrast to the pronounced differences in ultra-fine particle levels, the simulated number concentrations of particles in the CCN size range, approximated to 100-464 nm following the work of Sellegri et al. (2021), at 850 hPa remain of the same order of magnitude in the two simulations (Fig. 6.b). For most of the simulation period, the new nucleation scheme however produces concentrations up to twice those of the binary scheme, particularly during the first nucleation event discussed in Sect. 3.2.2. This suggests that the growth of particles formed at high altitudes may contribute to the formation of climatically significant sized-particles, in line with the literature.

From a chemical perspective, simulations indicate substantially higher nitric acid concentrations at higher altitudes (Fig. S6.a), with a median ratio of 37 compared to the surface, which likely explains the elevated $N_{1\text{-}10}$ concentrations simulated at 850 hPa (Fig. S6.c). This difference could result from enhanced photochemistry and reduced loss processes (given the high solubility of HNO_3) at altitude, or that HNO_3 derives from more efficient long-distance transport at higher altitudes. Sulfuric acid also shows a pronounced vertical contrast (Fig. S6.b), with concentrations at 850 hPa exceeding those in the lowest atmospheric levels by a median factor of 21, likely due to increased •HO availability driving the SO_2 oxidation pathway ($\bullet HO + SO_2 \rightarrow H_2SO_4$). Such vertical gradients are consistent with findings from boreal regions (Beck et al., 2022), although they contrast with observations from Réunion Island (Salignat et al., 2024), where sulfuric acid was found to be lower at altitude than near the surface; unfortunately, no nitric acid measurements were available in that study.

https://doi.org/10.5194/egusphere-2026-6891
Preprint. Discussion started: 19 November 2026
© Author(s) 2026. CC BY 4.0 License.

Overall, these results are promising but remain preliminary due to the lack of observation constraints at higher altitudes. Future airborne of high-elevation measurements in the marine free troposphere will be critical to validate this nucleation parameterization or to develop improved schemes tailored to higher altitudes, both for nucleation itself and for associated fluxes relevant to NPF processes.

Conclusions

In this study, we identified four new particle formation events triggered over the southwest Pacific Ocean, off the coast of New Zealand, using the marine-specific criterion proposed by Peltola et al. (2022). Although the aerosol size distributions were consistent with a marine environment, air mass back-trajectories revealed potential anthropogenic influences. Some of the air masses sampled during these events crossed regions such as Cook Strait, Wellington, or Christchurch, or traveled along the coast. Among the four events, we therefore selected only two for their marine signature, and both occurred during nighttime in frontal seawater, i.e., over the biologically active Chatham Rise region.

We tested and validated a new nucleation parameterization specifically designed for the remote marine atmosphere, based on the presence of nitric acid as a proxy for nitrate-driven nucleation (Salignat et al., accepted). This approach is grounded on the hypothesis proposed by Chamba et al. (2023), who suggest that nighttime nucleation may be driven by nitrate ions. The new parameterization was implemented in an optimized version of WRF-Chem, i.e., using the MOSAIC aerosol model extended to 12 bins (from 1 nm particles), including marine emissions of nitric oxide (as a precursor to HNO_3) and biogenic volatile organic compounds (such as isoprene and monoterpenes, which oxidation products contribute to the growth of newly formed particles).

Simulations of the two nighttime NPF events using the default WRF-Chem nucleation schemes, which rely on sulfuric acid concentrations, failed to reproduce the observed particle concentrations. The Binary scheme largely underestimated particle number concentrations, while the Activation scheme produced unrealistically high concentrations and failed to simulate nighttime NPF. In contrast, the new HNO_3-based parameterization successfully reproduced the temporal variability as well as the magnitude of the first marine NPF event. These results validate the potential of the new scheme to better capture nighttime marine NPF, compared to existing schemes in this region. However, the second event was not successfully reproduced. This may indicate that the nucleation was not nitrate-driven, or that it was influenced by dominant anthropogenic sources despite its partial marine classification. Further investigation, including the chemical analysis of particle composition, is needed to better constrain the driving mechanisms behind such events.

Overall, based on a single case study, it is not possible to draw definitive conclusions about the relevance of this nitrate-driven nucleation scheme for representing new particle formation in remote marine regions. Further evaluation is needed to assess whether this mechanism can reproduce observations from other remote oceanic remote regions and atmospheric layers (i.e., in particular the free troposphere). Other pathways, such as iodine oxoacid-driven nucleation during daytime, may also contribute to particle formation in the marine boundary layer (He et al., 2023) and represent an interesting direction for

https://doi.org/10.5194/egusphere-2026-6891
Preprint. Discussion started: 19 November 2026
© Author(s) 2026. CC BY 4.0 License.

future research in combination with nocturnal nitric acid nucleation. In addition, improved characterization of marine NO sources and a better understanding of the underlying biological and photochemical processes are needed, as uncertainties in these sources may influence the availability of nitric acid and, consequently, particle formation. Finally, it would be valuable to re-examine this case study using a model version that also incorporates both recent developments regarding primary biogenic particle formation processes (Rose et al., 2025), to enable an integrated assessment of the impact of primary and secondary sources on simulated concentrations.

Appendix A

In order to assess the impact of elevated nitric acid (HNO_3) concentrations on simulated nucleation rates, we performed several sensitivity tests in the WRF-Chem simulations (HNO_3 nucleation).

We first shortened the spin-up period from 144 to 60 hours, which increased the influence of anthropogenic nitric acid concentrations initialized at the beginning of the simulation. As a result, HNO_3 concentrations on average 2.6 times higher were simulated along the vessel's trajectory. Consequently, the parameterization predicted $N_{1\text{-}10}$ concentrations reaching up to 9239 particles.cm^{-3} during the March 19 event (Figure S4.a).

We then repeated the simulation using the same shortened spin-up but artificially limiting the nitric acid available for nucleation to roughly 2 x 10^7 molec.cm^{-3} (Figure S4.b), which roughly corresponds to the upper limit of the concentrations used to derive the nucleation parameterization. This led to slightly improved agreement with observations (RMSE = 360 particles.cm^{-3}), although particle concentrations were somewhat underestimated (on average 0.96 times lower than observations).

Code and data availability

Measurements of ambient particles performed throughout the Sea2Cloud campaign are available in the Sea2Cloud project data repository (Sea2Cloud Project, 2026) at https://sea2cloud.data-terra.org/en/catalogue/.

Author contributions

CR and KR supervised the project. CR, KS, and RS investigated and visualized the results. AL, CR, RS, and SB, curated the data and implemented the new developments in the model. CR, KS, and RS analysed the data and wrote the paper. All co-authors contributed to reviewing the paper.

https://doi.org/10.5194/egusphere-2026-6891
Preprint. Discussion started: 19 November 2026
© Author(s) 2026. CC BY 4.0 License.

Competing interests

The authors declare there are no conflicts of interest for this manuscript.

Acknowledgements

WRF-Chem simulations have been made on GENCI supercomputer (TGCC). The ERA5 meteorological data were provided by the following datasets: Hersbach et al. (2023a), DOI: https://doi.org/10.24381/cds.bd0915c6; and Hersbach et al. (2023b), DOI: https://doi.org/10.24381/cds.adbb2d47. The results contain modified Copernicus Climate Change Service information 2023. Neither the European Commission nor ECMWF is responsible for any use that may be made of the Copernicus information or data it contains. We would like to thank also Rahul Zaveri for his help on the implementation of the nucleation parameterization in the MOSAIC module.

Financial support

The research received funding from the European Research Council (ERC) under the Horizon 2020 (Grant Agreement 771369) and Horizon Europe (Grant Agreement 101115883) programmes, the Centre National des Etudes Spatiales (CNES). The Sea2Cloud project is endorsed by SOLAS. This project was provided with computer and storage resources by GENCI at TGCC thanks to the grants 2022- A0130111919 and 2023- A0150111919 on the supercomputer Joliot Curie's ROME partition.

References

Albrecht, B. A.: Aerosols, cloud microphysics, and fractional cloudiness, Science, 245(4923), 1227–1230, https://doi.org/10.1126/science.245.4923.1227, 1989.

Allan, J. D., Williams, P. I., Najera, J., Whitehead, J. D., Flynn, M. J., Taylor, J. W., Liu, D., Darbyshire, E., Carpenter, L. J., Chance, R., Andrews, S. J., Hackenberg, S. C., and McFiggans, G.: Iodine observed in new particle formation events in the Arctic atmosphere during ACCACIA, Atmos. Chem. Phys., 15, 5599–5609, https://doi.org/10.5194/acp-15-5599-2015, 2015.

Almeida, J., Schobesberger, S., Kürten, A., Ortega, I. K., Kupiainen-Määttä, O., Praplan, A. P., Adamov, A., Amorim, A., Bianchi, F., Breitenlechner, M., David, A., Dommen, J., Donahue, N. M., Downard, A., Dunne, E., Duplissy, J., Ehrhart, S., Flagan, R. C., Franchin, A., Guida, R., Hakala, J., Hansel, A., Heinritzi, M., Henschel, H., Jokinen, T., Junninen, H., Kajos, M., Kangasluoma, J., Keskinen, H., Kupc, A., Kurtén, T., Kvashin, A. N., Laaksonen, A., Lehtipalo, K., Leiminger, M., Leppä, J., Loukonen, V., Makhmutov, V., Mathot, S., McGrath, M. J., Nieminen, T., Olenius, T., Onnela, T., Petäjä, T., Riccobono, F., Riipinen, I., Rissanen, M., Rondo, L., Ruuskanen, T., Santos, F. D., Sarnela, N., Schallhart, S., Schnitzhofer,

https://doi.org/10.5194/egusphere-2026-6891
Preprint. Discussion started: 19 November 2026
© Author(s) 2026. CC BY 4.0 License.

R., Seinfeld, J. H., Simon, M., Sipilä, M., Stozhkov, Y., Stratmann, F., Tomé, A., Tröstl, J., Tsagkogeorgas, G., Vaattovaara, P., Viisanen, Y., Virtanen, A., Vrtala, A., Wagner, P. E., Weingartner, E., Wex, H., Williamson, C., Wimmer, D., Ye, P., Yli-Juuti, T., Carslaw, K. S., Kulmala, M., Curtius, J., Baltensperger, U., Worsnop, D. R., Vehkamäki, H., and Kirkby, J.: Molecular understanding of sulphuric acid-amine particle nucleation in the atmosphere, Nature, 502(7471), 359-363, https://doi.org/10.1038/nature12663, 2013.

Andreas, E.: Handbook of physical constants and functions for use in atmospheric boundary layer studies, Cold Regions Research and Engineering Laboratory, 2005.

Arkian, F., Thompson, C., Peischl, J., Bourgeois, I., Dibb, J., Jimenez, J. L., Campuzano-Jost, P., Li, J., Morey, S., McDonald, B. C., Wofsy, S., and Wang, S.: Nitrogen Oxides in the Remote Marine Environment: Implications for Oceanic Emissions and Photoloysis of Particulate Nitrate, Journal of Geophysical Research: Atmospheres, 130(22), https://doi.org/10.1029/2025JD044077, 2025.

Baccarini, A., Dommen, J., Lehtipalo, K., Henning, S., Modini, R. L., Gysel-Beer, M., Baltensperger, U., and Schmale, J.: Low volatility vapors and new particle formation over the southern ocean during the Antarctic circumnavigation expedition, Journal of Geophysical Research: Atmospheres, 126(22), https://doi.org/10.1029/2021JD035126, 2021.

Bates, T. S., Cline, J. D., Gammon, R. H., and Kelly-Hansen, S. R.: Regional and seasonal variations in the flux of oceanic dimethylsulfide to the atmosphere, Journal of Geophysical Research: Oceans, 92(C3), 2930–2938, https://doi.org/10.1029/JC092iC03p02930, 1987.

Beck, L. J., Sarnela, N., Junninen, H., Hoppe, C. J. M., Garmash, O., Bianchi, F., Riva, M., Rose, C., Peräkylä, O., Wimmer, D., Kausiala, O., Jokinen, T., Ahonen, L., Mikkilä, J., Hakala, J., He, X.-C., Kontkanen, J., Wolf, K. K. E., Cappelletti, D., Mazzola, M., Traversi, R., Petroselli, C., Viola, A. P., Vitale, V., Lange, R., Massling, A., Nøjgaard, J. K., Krejci, R., Karlsson, L., Zieger, P., Jang, S., Lee, K., Vakkari, V., Lampilahti, J., Thakur, R. C., Leino, K., Kangasluoma, J., Duplissy, E.-M., Siivola, E., Marbouti, M., Tham, Y. J., Saiz-Lopez, A., Petäjä, T., Ehn, M., Worsnop, D. R., Skov, H., Kulmala, M., Kerminen, V.-M., and Sipilä, M.: Differing mechanisms of new particle formation at two Arctic sites, Geophysical Research Letters, 48, e2020GL091334, https://doi.org/10.1029/2020GL091334, 2021.

Beck, L. J., Schobesberger, S., Junninen, H., Lampilahti, J., Manninen, A., Dada, L., Leino, K., He, X.-C., Pullinen, I., Quéléver, L. L. J., Franck, A., Poutanen, P., Wimmer, D., Korhonen, F., Sipilä, M., Ehn, M., Worsnop, D. R., Kerminen, V.-M., Petäjä, T., Kulmala, M., and Duplissy, J.: Diurnal evolution of negative atmospheric ions above the boreal forest: from ground level to the free troposphere, Atmos. Chem. Phys., 22, 8547–8577, https://doi.org/10.5194/acp-22-8547-2022, 2022.

Bellouin, N., Quaas, J., Gryspeerdt, E., Kinne, S., Stier, P., Watson-Parris, D., et al., Boucher, O., Carslaw, K. S., Christensen, M., Daniau, A.-L., Dufresne, J.-L., Feingold, G., Fiedler, S., Forster, P., Gettelman, A., Haywood, J. M., Lohmann, U., Malavelle, F., Mauritsen, T., McCoy, D. T., Myhre, G., Mülmenstädt, J., Neubauer, D., Possner, A., Rugenstein, M., Sato, Y., Schulz, M., Schwartz, S. E., Sourdeval, O., Storelvmo, T., Toll, V., Winker, D., and Stevens, B.: Bounding Global Aerosol Radiative Forcing of Climate Change, Review of Geophysics, 58(1), https://doi.org/10.1029/2019RG000660, 2020.

https://doi.org/10.5194/egusphere-2026-6891
Preprint. Discussion started: 19 November 2026
© Author(s) 2026. CC BY 4.0 License.

Berg, L. K., Shrivastava, M., Easter, R. C., Fast, J. D., Chapman, E. G., Liu, Y., and Ferrare, R. A.: A new WRF-Chem treatment for studying regional-scale impacts of cloud processes on aerosol and trace gases in parameterized cumuli, Geoscientific Model Development, 8, 409–429, https://doi.org/10.5194/gmd-8-409-2015, 2015.

Bock, J., Michou, M., Nabat, P., Abe, M., Mulcahy, J. P., Olivié, D. J. L., Schwinger, J., Suntharalingam, P., Tjiputra, J., van Hulten, M., Watanabe, M., Yool, A., and Séférian, R.: Evaluation of ocean dimethylsulfide concentration and emission in CMIP6 models, Biogeosciences, 18, 3823–3860, https://doi.org/10.5194/bg-18-3823-2021, 2021.

Brean, J., Dall'Osto, M., Simó, R. Shi, Z., Beddows, D., and Harrison, R. M.: Open ocean and coastal new particle formation from sulfuric acid and amines around the Antarctic Peninsula, Nature Geoscience, 14, 383–388, https://doi.org/10.1038/s41561-021-00751-y, 2021.

Brooks, S. D. and Thornton, D. C. O.: Marine Aerosols and Clouds, Annual Review of Marine Science, 10, 289-313, https://doi.org/10.1146/annurev-marine-121916-063148, 2018.

Carslaw, K. S., Lee, L. A., Reddington, C. L., Pringle, K. J., Rap, A., Forster, P. M., Mann, G. W., Spracklen, D. V., Woodhouse, M. T., Regayre, L. A., and Pierce, J. R.: Large contribution of natural aerosols to uncertainty in indirect forcing, Nature, 503(7474), 67-71, https://doi.org/10.1038/nature12674, 2013.

Carslaw, K. S., Gordon, H., Hamilton, D. S., Johnson, J. S., Regayre, L. A., Yoshioka, M., and Pringle, K. J.: Aerosols in the Pre-industrial Atmosphere, Current Climate Change Reports, 2017;3(1):1-15, https://doi.org/10.1007/s40641-017-0061-2, 2017.

Carter, W. P. L.: Documentation of the SAPRC-99 chemical mechanism for VOC reactivity assessment. Final Report to California Air Resources Board Contract 92-329 and Contract 95-308, Tech. rep., Air Pollution Research Center and College of Engineering Center for Environmental Research and Technology, University of California Riverside, California, 2000.

Chamba, G., Rissanen, M., Barthelmeβ, T., Saiz-Lopez, A., Rose, C., Iyer, S., Saint-Macary, A., Rocco, M., Safi, K., Deppeler, S., Barr, N., Harvey, M., Engel, A., Dunne, E., Law, C. S., and Sellegri, K.: Evidence of nitrate-based nighttime atmospheric nucleation driven by marine microorganisms in the South Pacific, Proceedings of the National Academy of Sciences, 120, 48, https://www.pnas.org/doi/abs/10.1073/pnas.2308696120, 2023.

Chang, R. Y.-W., Sjostedt, S. J., Pierce, J. R., Papakyriakou, T. N., Scarratt, M. G., Michaud, S., Levasseur, M., Leaitch, W. R., and Abbatt, J. P. D.: Relating atmospheric and oceanic DMS levels to particle nucleation events in the Canadian Arctic, Journal of Geophysical Research: Atmospheres, 116(D17), https://doi.org/10.1029/2011JD015926, 2011.

Charlson, R. J., Lovelock, J. E., Andreae, M. O., and Warren, S. G.: Oceanic phytoplankton, atmospheric sulphur, cloud albedo and climate, Nature, 326, 655–661, https://doi.org/10.1038/326655a0, 1987.

Chee, S., Myllys, N., Barsanti, K. C., Wong, B. M., and Smith, J. N.: An experimental and modeling study of nanoparticle formation and Growth from Dimethylamine and Nitric Acid, The Journal of Physical Chemistry, 123, 5640-5648, https://doi.org/10.1021/acs.jpca.9b03326, 2019.

https://doi.org/10.5194/egusphere-2026-6891
Preprint. Discussion started: 19 November 2026
© Author(s) 2026. CC BY 4.0 License.

Chen, D.-P., Ma, W., Yang, C.-H., Li, M., Zhou, Z.-Z., Zhang, Y., Wang, X.-C., and Quan, Z.-J.: Formation of atmospheric molecular clusters containing nitric acid with ammonia, methylamine, and dimethylamine, Environmental Science: Processes and Impacts, 26, 2036-2050, https://doi.org/10.1039/D4EM00330F, 2024.

Collins, D. B., Burkart, J., Chang, R. Y.-W., Lizotte, M., Boivin-Rioux, A., Blais, M., Mungall, E. L., Boyer, M., Irish, V. E., Massé, G., Kunkel, D., Tremblay, J.-É., Papakyriakou, T., Bertram, A. K., Bozem, H., Gosselin, M., Levasseur, M., and Abbatt, J. P. D.: Frequent ultrafine particle formation and growth in Canadian Arctic marine and coastal environments, Atmos. Chem. Phys., 17, 13119–13138, https://doi.org/10.5194/acp-17-13119-2017, 2017.

Dal Maso, M., Kulmala, M., Riipinen, I., Wagner, R., Hussein, T., Aalto, P., and Lehtinen, K.: Formation and growth of fresh atmospheric aerosols: eight years of aerosol size distribution data from SMEAR II, Hyytiälä, Finland, Boreal Environment Research, 10(5), 323-336, 2005.

Dall'Osto, M., Ceburnis, D., Monahan, C., Worsnop, D. R., Bialek, J., Kulmala, M., Kurtén, T., Ehn, M., Wenger, J., Sodeau, J., Healy, R., and O'Dowd, C.: Nitrogenated and aliphatic organic vapors as possible drivers for marine secondary organic aerosol growth, Journal of Geophysical Research: Atmospheres, 117(D12), https://doi.org/10.1029/2012JD017522, 2012.

Dudhia, J.: Numerical study of convection observed during the winter monsoon experiment using a mesoscale two-dimensional model, Journal of the Atmospheric Sciences, 46, 3077–3107, https://doi.org/10.1175/1520-0469(1989)046%3C3077:NSOCOD%3E2.0.CO;2, 1989.

Dunne, E. M., Gordon, H., Kürten, A., Almeida, J., Duplissy, J., Williamson, C., Ortega, I. K., Pringle, K. J., Adamov, A., Baltensperger, U., Barmet, P., Benduhn, F., Bianchi, F., Breitenlechner, M., Clarke, A., Curtius, J., Dommen, J., Donahue, N. M., Ehrhart, S., Flagan, R. C., Franchin, A., Guida, R., Hakala, J., Hansel, A., Heinritzi, M., Jokinen, T., Kangasluoma, J., Kirkby, J., Kulmala, M., Kupc, A., Lawler, M. J., Lehtipalo, K., Makhmutov, V., Mann, G., Mathot, S., Merikanto, J., Miettinen, P., Nenes, A., Onnela, A., Rap, A., Reddington, C. L. S., Riccobono, F., Richards, N. A. D., Rissanen, M. P., Rondo, L., Sarnela, N., Schobesberger, S., Sengupta, K., Simon, M., Sipilä, M., Smith, J. N., Stozkhov, Y., Tomé, A., Tröstl, J., Wagner, P. E., Wimmer, D., Winkler, P. M., Worsnop, D. R., and Carslaw, K. S.: Global atmospheric particle formation from CERN CLOUD measurements, Science, 354, 1119–1124, https://doi.org/10.1126/science.aaf2649, 2016.

Fast, J. D., Gustafson, W. I., Easter, R. C., Zaveri, R. A., Barnard, J. C., Chapman, E. G., Grell, G. A., and Peckham, S. E.: Evolution of ozone, particulates, and aerosol direct radiative forcing in the vicinity of Houston using a fully coupled meteorology chemistry-aerosol model, Journal of Geophysical Research: Atmosphere, 111, d21305, https://doi.org/10.1029/2005JD006721, 2006.

Fiddes, S. L., Woodhouse, M. T., Lane, T. P., and Schofield, R.: Coral-reef-derived dimethyl sulfide and the climatic impact of the loss of coral reefs, Atmospheric Chemistry and Physics, 21, 5883–5903, https://doi.org/10.5194/acp-21-5883-2021, 2021.

Fitzgerald, J. W.: Marine aerosols: A review, Atmospheric Environment, Part A. General Topics, 25(3-4), 533-545, https://doi.org/10.1016/0960-1686(91)90050-H, 1991.

https://doi.org/10.5194/egusphere-2026-6891
Preprint. Discussion started: 19 November 2026
© Author(s) 2026. CC BY 4.0 License.

Fuentes, E., Coe, H., Green, D., de Leeuw, G., and McFiggans, G.: On the impacts of phytoplankton-derived organic matter on the properties of the primary marine aerosol - Part 1: Source fluxes, Atmospheric Chemistry and Physics, 10(19), 9292-9317, https://doi.org/10.5194/acp-10-9295-2010, 2010.

Fuentes, E., Coe, H., Green, D., and McFiggans, G.: On the impacts of phytoplankton-derived organic matter on the properties of the primary marine aerosol – Part 2: Composition, hygroscopicity and cloud condensation activity, Atmospheric Chemistry and Physics, 11, 2585–2602, https://doi.org/10.5194/acp-11-2585-2011, 2011.

Gordon, H., Kirkby, J., Baltensperger, U., Bianchi, F., Breitenlechner, M., Curtius, J., Dias, A., Dommen, J., Donahue, N. M., Dunne, E. M., Duplissy, J., Ehrhart, S., Flagan, R. C., Frege, C., Fuchs, C., Hansel, A., Hoyle, C. R., Kulmala, M., Kürten, A., Lehtipalo, K., Makhmutov, V., Molteni, U., Rissanen, M. P., Stozkhov, Y., Tröstl, J., Tsagkogeorgas, G., Wagner, R., Williamson, C., Wimmer, D., Winkler, P. M., Yan, C., and Carslaw, K. S.: Causes and importance of new particle formation in the present-day and preindustrial atmospheres, J. Geophys. Res.-Atmos., 122, 8739–8760, https://doi.org/10.1002/2017jd026844, 2017.

Grell, G. A., Peckham, S. E., Schmitz, R., McKeen, S. A., Frost, G., Skamarock, W. C., and Eder, B.: Fully coupled "online" chemistry within the WRF model, Atmospheric Environment, 39, 6957–6975, https://doi.org/10.1016/j.atmosenv.2005.04.027, 2005.

He, X.-C., Simon, M., Iyer, S., Xie, H.-B., Rörup, B., Shen, J., Finkenzeller, H., Stolzenburg, D., Zhang, R., Baccarini, A., Tham, Y. J., Wang, M., Amanatidis, S., Piedehierro, A. A., Amorim, A., Baalbaki, R., Brasseur, Z., Caudillo, L., Chu, B., Dada, L., Duplissy, J., El Haddad, I., Flagan, R. C., Granzin, M., Hansel, A., Heinritzi, M., Hofbauer, V., Jokinen, T., Kemppainen, D., Kong, W., Krechmer, J., Kürten, A., Lamkaddam, H., Lopez, B., Ma, F., Mahfouz, N. G. A., Makhmutov, V., Manninen, H. E., Marie, G., Marten, R., Massabò, D., Mauldin, R. L., Mentler, B., Onnela, A., Petäjä, T., Pfeifer, J., Philippov, M., Ranjithkumar, A., Rissanen, M. P., Schobesberger, S., Scholz, W., Schulze, B., Surdu, M., Thakur, R. C., Tomé, A., Wagner, A. C., Wang, D., Wang, Y., Weber, S. K., Welti, A., Winkler, P. M., Zauner-Wieczorek, M., Baltensperger, U., Curtius, J., Kurtén, T., Worsnop, D. R., Volkamer, R., Lehtipalo, K., Kirkby, J., Donahue, N. M., Sipilä, M., and Kulmala, M.: Iodine oxoacids enhance nucleation of sulfuric acid particles in the atmosphere, Science, 382, 1308–1314, https://doi.org/10.1126/science.adh2526, 2023.

Hersbach, H., Bell, B., Berrisford, P., Biavati, G., Horányi, A., Muñoz Sabater, J., Nicolas, J., Peubey, C., Radu, R., Rozum, I., Schepers, D., Simmons, A., Soci, C., Dee, D., and Thépaut, J.-N.: ERA5 hourly data on pressure levels from 1940 to present [Dataset], Copernicus Climate Change Service (C3S) Climate Data Store (CDS), https://doi.org/10.24381/cds.bd0915c6, 2023a. (Accessed on 22-02-2021)

Hersbach, H., Bell, B., Berrisford, P., Biavati, G., Horányi, A., Muñoz Sabater, J., Nicolas, J., Peubey, C., Radu, R., Rozum, I., Schepers, D., Simmons, A., Soci, C., Dee, D., and Thépaut, J.-N.: ERA5 hourly data on single levels from 1940 to present [Dataset], Copernicus Climate Change Service (C3S) Climate Data Store (CDS), https://doi.org/10.24381/cds.adbb2d47, 2023b. (Accessed on 22-02-2021)

https://doi.org/10.5194/egusphere-2026-6891
Preprint. Discussion started: 19 November 2026
© Author(s) 2026. CC BY 4.0 License.

Hong, S., Noh, Y., and Dudhia, J.: A New Vertical Diffusion Package with an Explicit Treatment of Entrainment Processes, Monthly Weather Review, 134, 2318–2341, https://doi.org/10.1175/MWR3199.1, 2006.

Hulswar, S., Simó, R., Galí, M., Bell, T. G., Lana, A., Inamdar, S., Halloran, P. R., Manville, G., and Mahajan, A. S.: Third revision of the global surface seawater dimethyl sulfide climatology (DMS-Rev3), Earth Syst. Sci. Data, 14, 2963–2987, https://doi.org/10.5194/essd-14-2963-2022, 2022.

Jokinen, T., Sipilä, M., Kontkanen, J., Vakkari, V., Tisler, P., Duplissy, E.-M., Junninen, H., Kangasluoma, J., Manninen, H. E., Petäjä, T., Kulmala, M., Worsnop, D. R., Kirkby, J., Virkkula, A., and Kerminen, V.-M.: Ion-induced sulfuric acid–ammonia nucleation drives particle formation in coastal Antarctica, Science Advances, 4, eaat9744, https://doi.org/10.1126/sciadv.aat9744, 2018.

Kirkby, J., Curtius, J., Almeida, J., Dunne, E., Duplissy, J., Ehrhart, S., Franchin, A., Gagne, S., Ickes, L., Kurten, A., Kupc, A., Metzger, A., Riccobono, F., Rondo, L., Schobesberger, S., Tsagkogeorgas, G., Wimmer, D., Amorim, A., Bianchi, F., Breitenlechner, M., David, A., Dommen, J., Downard, A., Ehn, M., Flagan, R. C., Haider, S., Hansel, A., Hauser, D., Jud, W., Junninen, H., Kreissl, F., Kvashin, A., Laaksonen, A., Lehtipalo, K., Lima, J., Lovejoy, E. R., Makhmutov, V., Mathot, S., Mikkila, J., Minginette, P., Mogo, S., Nieminen, T., Onnela, A., Pereira, P., Petaja, T., Schnitzhofer, R., Seinfeld, J. H., Sipila, M., Stozhkov, Y., Stratmann, F., Tome, A., Vanhanen, J., Viisanen, Y., Vrtala, A., Wagner, P. E., Walther, H., Weingartner, E., Wex, H., Winkler, P. M., Carslaw, K. S., Worsnop, D. R., Baltensperger, U., and Kulmala, M.: Role of sulphuric acid, ammonia and galactic cosmic rays in atmospheric aerosol nucleation, Nature, 476, 429–433, https://doi.org/10.1038/nature10343, 2011.

Kerminen, V.-M., and Kulmala, M.: Analytical formulae connecting the “real” and the “apparent” nucleation rate and the nuclei number concentration for atmospheric nucleation events, Journal of Aerosol Science, 33(4), 609-622, https://doi.org/10.1016/s0021-8502(01)00194-x, 2002.

Kerminen, V.-M., Chen, X., Vakkari, V., Petäjä, T., Kulmala, M., and Bianchi, F.: Atmospheric new particle formation and growth: review of field observations, Environmental Research Letters, 13, 103003, https://doi.org/10.1088/1748-9326/aadf3c, 2018.

Kuang, C., McMurry, P. H., McCormick, A. V., and Eisele, F. L.: Dependence of nucleation rates on sulfuric acid vapor concentration in diverse atmospheric locations, Journal of Geophysical Research: Atmospheres, 113(D10), https://doi.org/10.1029/2007JD009253, 2008.

Kulmala, M., Kontkanen, J., Junninen, H., Lehtipalo, K., Manninen, H. E., Nieminen, T., Petäjä, T., Sipilä, M., Schobesberger, S., Rantala, P., Franchin, A., Jokinen, T., Järvinen, E., Äijälä, M., Kangasluoma, J., Hakala, J., Aalto, P. P., Paasonen, P., Mikkilä, J., Vanhanen, J., Aalto, J., Hakola, H., Makkonen, U., Ruuskanen, T., Mauldin, R. L., Duplissy, J., Vehkamäki, H., Bäck, J., Kortelainen, A., Riipinen, I., Kurtén, T., Johnston, M. V., Smith, J. N., Ehn, M., Mentel, T. F., Lehtinen, K. E. J., Laaksonen, A., Kerminen, V.-M., and Worsnop, D. R.: Direct Observations of Atmospheric Aerosol Nucleation, Science, 339, 943– 946, https://doi.org/10.1126/science.1227385, 2013.

https://doi.org/10.5194/egusphere-2026-6891
Preprint. Discussion started: 19 November 2026
© Author(s) 2026. CC BY 4.0 License.

Kulmala, M., and Laaksonen, A.: Binary nucleation of water-sulfuric acid system: Comparison of classical theories with different H_2SO_4 saturation vapor pressures, The Journal of Chemical Physics, 93, 696-701, https://doi.org/10.1063/1.459519, 1990.

Kulmala, M., Lehtinen, K. E. J., and Laaksonen, A.: Cluster activation theory as an explanation of the linear dependence between formation rate of 3nm particles and sulphuric acid concentration, Atmospheric Chemistry and Physics, 6(3), 787-793, https://doi.org/10.5194/acp-6-787-2006, 2006.

Kulmala, M, Vehkamäki, H., Petäjä, T., Dal Maso, M., Lauri, A., Kerminen, V.-M., Birmili, W., and McMurry, P. H.: Formation and growth rates of ultrafine atmospheric particles: a review of observations, Journal of Aerosol Science, 35(2), 143-176, https://doi.org/10.1016/j.jaerosci.2003.10.003, 2004.

Lee, S.-H., Gordon, H., Yu, H., Lehtipalo, K., Haley, R., Li, Y., and Zhang, R.: New particle formation on the atmosphere: From molecular clusters to global climate, Journal of Geophysical Research: Atmospheres, 124, 7098-7146, https://doi.org/10.1029/2018JD029356, 2019.

Lucas, D. D., and Akimoto, H.: Evaluating aerosol nucleation parameterizations in a global atmospheric model, Geophysical Research Letters, 33, L10808, https://doi.org/10.1029/2006GL025672, 2006.

Lupascu, A., Easter, R., Zaveri, R., Shrivastava, M., Pekour, M., Tomlinson, J., Yang, Q., Matsui, H., Hodzic, A., Zhang, Q., and Fast, J. D.: Modeling particle nucleation and growth over northern California during the 2010 CARES campaign, Atmos. Chem. Phys., 15, 12283–12313, https://doi.org/10.5194/acp-15-12283-2015, 2015.

Määttänen, A., Merikanto, J., Henschel, H., Duplissy; J., Makkonen, R., Ortega, I. K., and Vehkamäki, H.: New parameterizations for neutral and ion-induced sulphuric acid-water particle formation in nucleation and kinetic regimes, Journal of Geophysical Research: Atmospheres, 107(D19), https://doi.org/10.1002/2017JD027429, 2018.

Marelle, L., Raut, J.-C., Law, K. S., Berg, L. K., Fast, J. D., Easter, R. C., Shrivastava, M., and Thomas, J. L.: Improvements to the WRF-Chem 3.5.1 model for quasi-hemispheric simulations of aerosols and ozone in the Arctic, Geosci. Model Dev., 10, 3661–3677, https://doi.org/10.5194/gmd-10-3661-2017, 2017.

McGillis, W. R., Dacey, J. W. H., Frew, N. M., Bock, E. J., and Nelson, R. K.: Water-air flux of dimethylsulfide, Journal of Geophysical Research: Oceans, 105(C1), 1187-1193, https://doi.org/10.1029/1999jc900243, 2000.

Merikanto, J., Napari, I., Vehkamäki, H., Anttila, T., and Kulmala, M.: New parameterization of sulfuric acid-ammonia-water ternary nucleation rates at tropospheric conditions, Journal of Geophysical Research: Atmospheres, 112(D15), https://doi.org/10.1029/2006JD007977, 2007.

Merikanto, J., Spracklen, D. V., Mann, G. W., Pickering, S. J., and Carslaw, K. S.: Impact of nucleation on global CCN, Atmospheric Chemistry and Physics, 9, 8601-8616, https://doi.org/10.5194/acp-9-8601-2009, 2009.

Mlawer, E. J., Taubman, S. J., Brown, P. D., Iacono, M. J. and Clough, S. A.: Radiative transfer for inhomogeneous atmospheres: RRTM, avalidated correlated-k model for the longwave, Journal of Geophysical Research: Atmospheres, 102,16,663 – 16,682, https://doi.org/10.1029/97JD00237, 1997.

https://doi.org/10.5194/egusphere-2026-6891
Preprint. Discussion started: 19 November 2026
© Author(s) 2026. CC BY 4.0 License.

Morrison, H., Thompson, G., and Tatarskii, V.: Impact of Cloud Microphysics on the Development of Trailing Stratiform Precipitation in a Simulated Squall Line: Comparison of One- and Two-Moment Schemes, Monthly Weather Review, 137, 991–1007, https://doi.org/10.1175/2008MWR2556.1, 2009.

Napari, I., Noppel, M., Vehkamäki, H., and Kulmala, M.: Parameterization of ternay nucleation rates for H_2SO_4-NH_3-H_2O vapors, Journal of Geophysical Research: Atmospheres, 107(D19), https://doi.org/10.1029/2002JD002132, 2002.

Nightingale, P. D., Malin, G., Law, C. S., Watson, A. J., Liss, P. S., Liddicoat, M. I., Boutin, J., and Upstill-Goddard, R. C.: In-situ evaluation of air-sea gas exchange parameterizations using novel conservative and volatile tracers, Global Biogeochemical Cycles, 14(1), 373-387, https://doi.org/10.1029/1999gb900091, 2000.

O'Dowd, C. D., Hämeri, K., Mäkelä, J. M., Pirjola, L., Kulmala, M., Jennings, S. G., Berresheim, H., Hansson, H.-C., De Leeuw, G., Kunz, G. J., Allen, A. G., Hewitt, C. N., Jackson, A., Vilsanen, Y., and Hoffmann, T.: A dedicated study of New Particle Formation and Fate in the Coastal Environment (PARFORCE): Overview of objectives and achievements, Journal of Geophysical research: Atmospheres, 107(D19), https://doi.org/10.1029/2001JD000555, 2002.

O'Dowd, C. D., Monahan, C., and Dall'Osto, M.: On the occurrence of open ocean particle production and growth events, Geophysical Research Letters, 37(19), https://doi.org/10.1029/2010GL044679, 2010.

Palmer, P. I., and Shaw, S. L.: Quantifying global marine isoprene fluxes using MODIS chlorophyll observations, Geophysical Research Letters, 32(9), https://doi.org/10.1029/2005gl022592, 2005.

Peltola, M.: Marine biogeochemical emissions and aerosol formation, Earth Sciences, Université Clermont Auvergne, 2021.

Peltola, M., Rose, C., Trueblood, J. V., Gray, S., Harvey, M., and Sellegri, K.: New particle formation in coastal New Zealand with a focus on open-ocean air masses, Atmospheric Chemistry and Physics, 22(9), 6231-6254, https://doi.org/10.5194/acp-22-6231-2022, 2022.

Peltola, M., Rose, C., Trueblood, J. V., Gray, S., Harvey, M., and Sellegri, K.: Chemical precursors of new particle formation in coastal New Zealand, Atmospheric Chemistry and Physics, 23, 3955–3983, https://doi.org/10.5194/acp-23-3955-2023, 2023.

Petters, M. D., Snider, J. R., Stevens, B., Vali, G., Faloona, I. and Russel, L. M.: Accumulation mode aerosol, pockets of open cells, and particle nucleation in the remote subtropical Pacific marine boundary layer, Journal of Geophysical Research, 111, D02206, https://doi.org/10.1029/2004JD005694, 2006.

Pirjola, L., O'Dowd, C. D., Brooks, I. M., and Kulmala, M.: Can new particle formation occur in the clean marine boundary layer? Journal of Geophysical Research: Atmospheres, 105(D21), 26531-26546, https://doi.org/10.1029/2000JD900310, 2000.

Quinn, P. K. and Bates, T. S.: The case against climate regulation via oceanic phytoplankton sulphur emissions, Nature, 480, 5156, https://doi.org/10.1038/nature10580, 2011.

Riipinen, I., Sihto, S.-L., Kulmala, M., Arnold, F., Dal Maso, M., Birmili, W., Saarnio, K., Teinilä, K., Kerminen, V.-M., Laaksonen, A., and Lehtinen, K. E. J.: Connections between atmospheric sulphuric acid and new particle formation during

https://doi.org/10.5194/egusphere-2026-6891
Preprint. Discussion started: 19 November 2026
© Author(s) 2026. CC BY 4.0 License.

QUEST III–IV campaigns in Heidelberg and Hyytiälä, Atmos. Chem. Phys., 7, 1899–1914, https://doi.org/10.5194/acp-7-1899-2007, 2007.

Rolph, G., Stein, A., and Stunder, B: Real-time Environmental Applications and Display sYstem: Ready, Environmental Modelling & Software, 95, 210-228, https://doi.org/10.1016/j.envsoft.2017.06.025, 2017.

Rocco, M., Dunne, E., Salignat, R., Saint-Macary, A., Peltola, M., Barthelmess, T., et al. : Relating dimethyl sulphide and methanethiol fluxes to surface biota in the south-west Pacific using shipboard air-sea interface tanks. Journal of Geophysical Research: Atmospheres, 130, e2024JD041072. https://doi.org/10.1029/2024JD041072, 2025a.

Rocco, M., Dunne, E., Peltola, M., Barthelmess, T., Salignat, R., Chamba, G., Barr, N., Safi, K., Marriner, A., Deppeler, S., Rose, C., Uitz, J., Harnwell, J., Engel, A., Colomb, A., Saiz-Lopez, A., Harvey, M. J., Law, C. S., and Sellegri, K.: Fluxes of Biogenic and Oxygenated VOCs from in-situ Mesocosm Studies of Seawaters from the South-West Pacific Ocean, Journal of Geophysical Research: Atmospheres, 130, e2024JD043056, https://doi.org/10.1029/2024JD043056, 2025b.

Rose, C., Sellegri, K., Asmi, E., Hervo, M., Freney, E., Colomb, A., Junninen, H., Duplissy, J., Sipilä, M., Kontkanen, J., Lehtipalo, K., and Kulmala, M.: Major contribution of neutral clusters to new particle formation at the interface between the boundary layer and the free troposphere, Atmos. Chem. Phys., 15, 3413–3428, https://doi.org/10.5194/acp-15-3413-2015, 2015.

Rose, C., Banson, S., Planche, C., Lupascu, A., Salignat, R., Delanoë, J., Uitz, J., Peyrin, F., Donnadieu, F., Law, C. S., and Sellegri, K.: Impact of seawater biological activity on sea spray aerosols (SSA) number concentration and cloud properties in WRF-Chem – Case studies on the Southern Ocean, Journal of Geophysical Research: Atmospheres, 130, e2024JD042088, https://doi.org/10.1029/2024JD042088, 2025.

Russel, L., Moore, R., Burrows, S., and Quinn, P.: Ocean flux of salt, sulfate, and organic components to atmospheric aerosol, Earth-Science Reviews, 239, 104364, https://doi.org/10.1016/j.earscirev.2023.104364, 2023.

Salignat, R., Rissanen, M., Iyer, S., Baray, J.-L., Tulet, P., Metzger, J.-M., Brioude, J., Sellegri, K., and Rose, C.: Measurement report: Insights into the chemical composition and origin of molecular clusters and potential precursor molecules present in the free troposphere over the southern Indian Ocean: observations from the Maïdo Observatory (2150 m a.s.l., Réunion), Atmos. Chem. Phys., 24, 3785–3812, https://doi.org/10.5194/acp-24-3785-2024, 2024.

Salignat, R., Rose, C., Banson, S., Berthet, S., Lupascu, A., Uitz, J., Mallet, M., Seferian, R., Rocco, M., Colomb, A., Dunne, E., Saint-Macary, A., Marriner, A., Law, C.S., and Sellegri, K.: Sensitivity study of atmospheric DMS simulated in WRF-Chem to various oceanic DMS fields over the south west Pacific, Journal of Geophysical Research: Atmospheres, 130, e2024JD042271, https://doi.org/10.1029/2024JD042271, 2025.

Salignat, R., Chamba, G., Pailler, L., Colomb, A., Leriche, M., Deguillaume, L., Rose, C., and Sellegri, K.: New Insights into Nighttime Marine Sulfur and Nitrogen Chemistry and Related new Particle Formation Using the CLEPS model, Journal of Geophysical Research: Atmospheres, 131, e2025JD044824, https://doi.org/10.1029/2025JD044824, 2026.

Sander, R.: Compilation of Henry's law constants (version 5.0.0) for water as solvent, Atmospheric Chemistry and Physics, 23, 10901–12440, https://doi.org/10.5194/acp-23-10901-2023, 2023.

https://doi.org/10.5194/egusphere-2026-6891
Preprint. Discussion started: 19 November 2026
© Author(s) 2026. CC BY 4.0 License.

Schwier, A. N., Rose, C., Asmi, E., Ebling, A. M., Landing, W. M., Marro, S., Pedrotti, M.-L., Sallon, A., Iuculano, F., Agusti, S., Tsiola, A., Pitta, P., Louis, J., Guieu, C., Gazeau, F., and Sellegri, K.: Primary marine aerosol emissions from the Mediterranean Sea during pre-bloom and oligotrophic conditions: correlations to seawater chlorophyll *a* from a mesocosm study, Atmos. Chem. Phys., 15, 7961–7976, https://doi.org/10.5194/acp-15-7961-2015, 2015.

Schwier, A. N., Sellegri, K., Mas, S., Charrière, B., Pey, J., Rose, C., Temime-Roussel, B., Jaffrezo, J.-L., Parin, D., Picard, D., Ribeiro, M., Roberts, G., Sempéré, R., Marchand, N., and D'Anna, B.: Primary marine aerosol physical flux and chemical composition during a nutrient enrichment experiment in mesocosms in the Mediterranean Sea, Atmos. Chem. Phys., 17, 14645–14660, https://doi.org/10.5194/acp-17-14645-2017, 2017.

Sea2Cloud Project: Sea2Cloud campaign measurements repository [Dataset]. Sea2Cloud DATA TERRA. https://sea2cloud.data-terra.org/en/catalogue/, 2026. (Accessed on 21-05-2026)

Séférian, R., Nabat, P., Michou, M., Saint-Martin, D., Voldoire, A., Colin, J., Decharme, B., Delire, C., Berthet, S., Chevallier, M., Sénési, S., Franchisteguy, L., Vial, J., Mallet, M., Joetzjer, E., Geoffroy, O., Guérémy, J.-F., Moine, M.-P., Msadek, R., Ribes, A., Rocher, M., Roehrig, R., Salas-y-Mélia, D., Sanchez, E., Terray, L., Valcke, S., Waldman, R., Aumont, O., Bopp, L., Deshayes, J., Éthé, C., and Madec, G.: Evaluation of CNRM Earth-System model, CNRM-ESM2-1: role of Earth system processes in present-day and future climate, Journal of Advances in Modeling Earth Systems, 11, 4182–4227, https://doi.org/10.1029/2019MS001791, 2019.

Sellegri, K., Nicosia, A., Freney, E., Uitz, J., Thyssen, M., Grégori, G., Engel, A., Zäncker, B., Haëntjens, N., Mas, S., Picard, D., Saint-Macary, A., Peltola, M., Rose, C., Trueblood, J., Lefevre, D., D'Anna, B., Desboeufs, K., Meskhidze, N., Guieu, C., and Law, C. S.: Surface ocean microbiota determine cloud precursors, Scientific Reports, 11(1), https://doi.org/10.1038/s41598-020-78097-5, 2021.

Sellegri, K., Harvey, M., Peltola, M., Saint-Macary, A., Barthelmeß, T., Rocco, M., Moore, K. A., Cristi, A., Peyrin, F., Barr, N., Labonnote, L., Marriner, A., McGregor, J., Safi, K., Deppeler, S., Archer, S., Picard, D., Dunne, E., Harnwell, J., Delanoe, J., Colomb, A., Freney, E., Saiz Lopez, A., QuintanillaLópez, J. E., Lebrón-Aguilar, R., Rinaldi, M., Banson, S., Rose, C., Planche, C., Joseph, R., Lupascu, A., Jourdan, O., Mioche, G., Olivares, G., Querel, R., McDonald, A., Plank, G., Dillon, W., Blarel, L., Pelon, J., Donnadieu, F., Tridon, F., Baray, J.-L., Szczap, F., Engel, A., DeMott, P. J., and Law, C.: Sea2Cloud: From Biogenic Emission Fluxes to Cloud Properties in the Southwest Pacific, Bulletin of the American Meteorological Society, 104(5), E1017-E1043, https://doi.org/10.1175/BAMS-D-21-0063.1, 2023a.

Sellegri, K., Barthelmeß, T., Trueblood, J., Cristi, A., Freney, E., Rose, C., Barr, N., Harvey, M., Safi, K., Deppeler, S., Thompson, K., Dillon, W., Engel, A., and Law, C.: Quantified effect of seawater biogeochemistry on the temperature dependence of sea spray aerosol fluxes, Atmos. Chem. Phys., 23, 12949–12964, https://doi.org/10.5194/acp-23-12949-2023, 2023b.

Semeniuk, K., and Dastoor, A.: Current state of aerosol nucleation parameterizations for air-quality and climate modeling, Atmospheric Environment, 179, 77-106, https://doi.org/10.1016/j.atmosenv.2018.01.039, 2018.

https://doi.org/10.5194/egusphere-2026-6891
Preprint. Discussion started: 19 November 2026
© Author(s) 2026. CC BY 4.0 License.

Shen, Y., Wang, J., Gao, Y., Chan, C. K., Zhu, Y., Gao, H., Petäjä, T., and Yao, X.: Sources and formation of nucleation mode particles in remote tropical marine atmospheres over the South China Sea and the Northwest Pacific Ocean, Science of The Total Environment, 735(15), https://doi.org/10.1016/j.scitotenv.2020.139302, 2020.

Shrivastava, M., Fast, J., Easter, R., Gustafson Jr., W. I., Zaveri, R. A., Jimenez, J. L., Saide, P., and Hodzic, A.: Modeling organic aerosols in a megacity: comparison of simple and complex representations of the volatility basis set approach, Atmos. Chem. Phys., 11, 6639–6662, https://doi.org/10.5194/acp-11-6639-2011, 2011.

Sihto, S.-L., Kulmala, M., Kerminen, V.-M., Dal Maso, M., Petäjä, T., Riipinen, I., Korhonen, H., Arnold, F., Janson, R., Boy, M., Laaksonen, A., and Lehtinen, K. E. J.: Atmospheric sulphuric acid and aerosol formation: implications from atmospheric measurements for nucleation and early growth mechanisms, Atmos. Chem. Phys., 6, 4079–4091, https://doi.org/10.5194/acp-6-4079-2006, 2006.

Sipilä, M., Berndt, T., Petäjä, T., Brus, D., Vanhanen, J., Stratmann, F., Patokoski, J., Mauldin, R. L., Hyvärinen, A.-P., Lihavainen, H., and Kulmala, M.: The role of sulphuric acid in atmospheric nucleation, Science, 327(5970), 1243-1246. https://doi.org/10.1126/science.1180315, 2010.

Sipilä, M., Sarnela, N., Jokinen, T., Henschel, H., Junninen, H., Kontkanen, J., Richters, S., Kangasluoma, J., Franchin, A., Peräkylä, O., Rissanen, M. P., Ehn, M., Vehkamäki, H., Kurten, T., Berndt, T., Petäjä, T., Worsnop, D., Ceburnis, D., Kerminen, V.-M., Kulmala, M., and O'Dowd, C.: Molecular-scale evidence of aerosol particle formation via sequential addition of HIO_3, Nature, 537, 532-534, https://doi.org/10.1038/nature19314, 2016.

Song, A., Li, J., Tsona, N.T., and Du, L.: Parameterizations for sea spray aerosol production flux, Applied Geochemistry, 157, 105776, https://doi.org/10.1016/j.apgeochem.2023.105776, 2023.

Spracklen, D. V., Pringle, K. J., Carslaw, K. S., Chipperfield, M. P., and Mann, G. W.: A global off-line model of size-resolved aerosol microphysics: I. Model development and prediction of aerosol properties, Atmospheric Chemistry and Physics, 5(8), 2227-2252, https://doi.org/10.5194/acp-5-2227-2005, 2005.

Spracklen, D. V., Carslaw, K. S., Merikanto, J., Mann, G. W., Reddington, C. L., Pickering, S., Ogren, J. A., Andrews, E., Baltensperger, U., Weingartner, E., Boy, M., Kulmala, M., Laakso, L., Lihavainen, H., Kivekäs, N., Komppula, M., Mihalopoulos, N., Kouvarakis, G., Jennings, S. G., O'Dowd, C., Birmili, W., Wiedensohler, A., Weller, R., Gras, J., Laj, P., Sellegri, K., Bonn, B., Krejci, R., Laaksonen, A., Hamed, A., Minikin, A., Harrison, R. M., Talbot, R., and Sun, J.: Explaining global surface aerosol number concentrations in terms of primary emissions and particle formation, Atmos. Chem. Phys., 10, 4775–4793, https://doi.org/10.5194/acp-10-4775-2010, 2010.

Stein, A. F., Draxler, R. R., Rolph, G. D., Stunder, B. J. B., Cohen, M. D., and Ngan, F.: NOAA's HYSPLIT Atmospheric Transport and Dispersion Modeling System, Bulletin of the American Meteorological Society, 96(16), 2059-2077, https://doi.org/10.1175/bams-d-14-00110.1, 2015.

Tian, Y., Yang, G.-P., Liu, C.-Y., Li, P.-F., Chen, H.-T., and Bange, H. W.: Photoproduction of nitric oxide in seawater, Ocean Science, 16(1), 135-148, https://doi.org/10.5194/os-16-135-2020, 2020.

https://doi.org/10.5194/egusphere-2026-6891
Preprint. Discussion started: 19 November 2026
© Author(s) 2026. CC BY 4.0 License.

Twomey, S.: The influence of pollution on the shortwave albedo of clouds, Journal of the Atmospheric Sciences, 34(7), 1149–1152, https://doi.org/10.1175/1520-0469(1977)034<1149:TIOPOT>2.0.CO;2, 1977.

Ueda, S., Miura, K., Kawata, R., Furutani, H., Uematsu, M., Omori, Y., and Tanimoto, H.: Number-size distribution of aerosol particles and new particles formation events in tropical and sub-tropical Pacific Oceans, Atmospheric Environment, 142, 324-339, https://doi.org/10.1016/j.atmosenv.2016.07.055, 2016.

Uitz, J., Claustre, H., Morel, A., and Hooker, S. B.: Vertical distribution of phytoplankton communities in open ocean: An assessment based on surface chlorophyll, Journal of Geophysical Research: Oceans, 111, C08005, https://doi.org/10.1029/2005JC003207, 2006.

Vanhanen, J., Mikkilä, J., Lehtipalo, K., Sipilä, M., Manninen, H. E., Siivola, E., Petäjä, T., and Kulmala, M.: Particle Size Magnifier for Nano-CN Detection, Aerosol Science and Technology, 45(4), 533-542, https://doi.org/10.1080/02786826.2010.547889, 2011.

Vehkamäki, H., Kulmala, M., Napari, I., Lehtinen, K. E. J., Timmreck, C., Noppel, M., and Laaksonen, A.: An improved parameterization for sulfuric acid-water nucleation rates for tropospheric and stratospheric conditions, Journal of Geophysical Research: Atmospheres, 107(D22), 4622, https://doi.org/10.1029/2002JD002184, 2022.

Wang, M. and Penner, J. E.: Aerosol indirect forcing in a global model with particle nucleation, Atmos. Chem. Phys., 9, 239–260, https://doi.org/10.5194/acp-9-239-2009, 2009.

Wang, M., Xiao, M., Bertozzi, B., Marie, G., Rörup, B., Schulze, B., Bardakov, R., He, X.-C., Shen, J., Scholz, W., Marten, R., Dada, L., Baalbaki, R., Lopez, B., Lamkaddam, H., Manninen, H. E., Amorim, A., Ataei, F., Bogert, P., Brasseur, Z., Caudillo, L., De Menezes, L.-P., Duplissy, J., Ekman, A. M. L., Finkenzeller, H., Carracedo, L. G., Granzin, M., Guida, R., Heinritzi, M., Hofbauer, V., Höhler, K., Korhonen, K., Krechmer, J. E., Kürten, A., Lehtipalo, K., Mahfouz, N. G. A., Makhmutov, V., Massabò, D., Mathot, S., Mauldin, R. L., Mentler, B., Müller, T., Onnela, A., Petäjä, T., Philippov, M., Piedehierro, A. A., Pozzer, A., Ranjithkumar, A., Schervish, M., Schobesberger, S., Simon, M., Stozhkov, Y., Tomé, A., Umo, N. S., Vogel, F., Wagner, R., Wang, D. S., Weber, S. K., Welti, A., Wu, Y., Zauner-Wieczorek, M., Sipilä, M., Winkler, P. M., Hansel, A., Baltensperger, U., Kulmala, M., Flagan, R. C., Curtius, J., Riipinen, I., Gordon, H., Lelieveld, J., El-Haddad, I., Volkamer, R., Worsnop, D. R., Christoudias, T., Kirkby, J., Möhler, O., and Donahue, N. M.: Synergistic HNO3–H2SO4–NH3 upper tropospheric particle formation, Nature, 605, 483–489, https://doi.org/10.1038/s41586-022-04605-4, 2022.

Weber, R. J., McMurry, P. H., Mauldin III, R. L., Tanner, D. J., Eisele, F. L., Clarke, A. D., and Kapustin, V. N.: New particle formation in the remote troposphere: A comparison of observations at various sites, Geophysical Research Letters, 26, 307-310, https://doi.org/10.1029/1998GL900308, 1999.

Wexler, A. S., Lurmann, F. W., and Seinfeld, J. H.: Modelling urban and regional aerosols – I. model development, Atmospheric Environment, 28(3), 531-546, https://doi.org/10.1016/1352-2310(94)90129-5, 1994.

Wiedensohler, A., Birmili, W., Nowak, A., Sonntag, A., Weinhold, K., Merkel, M., Wehner, B., Tuch, T., Pfeifer, S., Fiebig, M., Fjäraa, A. M., Asmi, E., Sellegri, K., Depuy, R., Venzac, H., Villani, P., Laj, P., Aalto, P., Ogren, J. A., Swietlicki, E.,

https://doi.org/10.5194/egusphere-2026-6891
Preprint. Discussion started: 19 November 2026
© Author(s) 2026. CC BY 4.0 License.

Williams, P., Roldin, P., Quincey, P., Hüglin, C., Fierz-Schmidhauser, R., Gysel, M., Weingartner, E., Riccobono, F., Santos, S., Grüning, C., Faloon, K., Beddows, D., Harrison, R., Monahan, C., Jennings, S. G., O'Dowd, C. D., Marinoni, A., Horn, H.-G., Keck, L., Jiang, J., Scheckman, J., McMurry, P. H., Deng, Z., Zhao, C. S., Moerman, M., Henzing, B., de Leeuw, G., Löschau, G., and Bastian, S.: Mobility particle size spectrometers: harmonization of technical standards and data structure to facilitate high quality long-term observations of atmospheric particle number size distributions, Atmos. Meas. Tech., 5, 657–685, https://doi.org/10.5194/amt-5-657-2012, 2012.

Wild, O., Zhu, X., and Prather, M. J.: Fast-J: Accurate Simulation of In- and Below-Cloud Photolysis in Tropospheric Chemical Models, Journal of Atmospheric Chemistry, 37, 245–282, https://doi.org/10.1023/A:1006415919030, 2000.

Wise D., and Houghton, G.: Diffusion coefficients of neon, krypton, xenon, carbon monoxide and nitric oxide in water at 10-60°C. Chemical Engineering Science, 23(10), 1211-1216, https://doi.org/10.1016/0009-2509(68)89029-3, 1968.

Yoon, Y. J., Ceburnis, D., Cavalli, F., Jourdan, O., Putaud, J. P., Facchini, M. C., Decesari, S., Fuzzi, S., Sellegri, K., Jennings, S. G., and O'Dowd, C. D.: Seasonal characteristics of the physiochemical properties of north Atlantic marine atmospheric aerosols, Journal of Geophysical Research: Atmospheres, 112(D4), https://doi.org/10.1029/2005JD007044, 2007.

Yu, F., Luo, G., Bates, T. S., Anderson, B., Clarke, A., Kapustin, V., Yantosca, R. M., Wang, Y., and Wu, S.: Spatial distributions of particle number concentrations in the global troposphere: Simulations, observations, and implications for nucleation mechanisms, Journal of Geophysical Research: Atmospheres, 115(D17), https://doi.org/10.1029/2009JD013473, 2010.

Zaveri, R. A., Easter, R. C., Fast, J. D., and Peters, L. K.: Model for Simulating Aerosol Interactions and Chemistry (MOSAIC), Journal of Geophysical Research: Atmospheres, 113, d13204, https://doi.org/10.1029/2007JD008782, 2008.